2006

Development of a small separation riser for fine coal particles

Haroon Akhtar
West Virginia University

Development of a Small Separation Riser for Fine Coal Particles.

Haroon Akhtar

Thesis

Submitted to the College of Engineering and Mineral Resources

at West Virginia University

in partial fulfillment of the requirements
for the degree of

Master of Science

in

Mechanical Engineering

Eric Johnson, P.h.D., Chair
Bruce Kang, P.h.D.
Frank L. Saus, P.h.D.

Department of Mechanical Engineering

Morgantown

West Virginia

2006

Keywords: Fluidization, Fine coal, Riser, Cyclone.

ABSTRACT

Development of a Small Separation Riser for Fine Coal Particles

Haroon Akhtar

The wet, density based, separation processes employed at the coal preparation plant do not deal with particles under the size of 150 micrometers, resulting in the waste of precious coal resources. An exploratory fluidized bed riser system was developed to separate pyrite from fine coal particles under 150 micrometers in diameter. Gas velocity U_0 and solid mass flux G_p were the controlled variables so that the flow pattern within the riser was in the transition region from fast fluidization to dilute regime. Nine tests were conducted using coal and nine tests were conducted using a mixture of 10% iron and 90% coal by mass so as to study the effect of iron particles on the separation of pyrite from coal. Different feeder configurations for injecting solid particles in the riser were also employed in this study and their performance was compared. The separation of pyrite from coal was insignificant for the conditions employed in the study.

TABLE OF CONTENTS

LIST OF FIGURES

LIST OF TABLES

LIST OF SYMBOLS

a	Strength of intermolecular forces
A	Hamaker's constant
A_r	Archimedes Number
B	Finite volume occupied by the gas
B_c	Width of cyclone inlet
d_p	Diameter of particle
D_c	Diameter of cyclone
D_e	Air outlet diameter from the cyclone
e	Charge on an electron
E	Non retarded energy of interaction
G	Solid flow rate
G_p	Solid mass flux
h	Planks Constant
H	Inter-atomic distance
H_v	Ratio of stresses near the vertical wall
J_c	Diameter of solid outlet from the cyclone
K	Boltzman's constant
Lc	Length of main cylinder of cyclone
m_e	Mass of electron
N	Number of turns in cyclone
N_A	Number of electrons in atom A
N_B	Number of electrons in atom B

P	Pressure
R	Inter-atomic distance
R_e	Reynolds number
R_{et}	Reynolds number at terminal velocity
S_c	Height of inlet above cyclone air outlet
U_o	Superficial velocity
U_{mf}	Minimum fluidization velocity
U_{fd}	Upper bound for gas velocity for fast fluidization
U_{pt}	Terminal velocity of particles
U_{tf}	Lower bound for gas velocity for fast fluidization
V_i	Cyclone inlet velocity
Z_c	Length of cone in the cyclone

GREEK

α	Zero frequency polarizability of a molecule
Δ	Change
ρ	Density
ρ_g	Gas density
ρ_p	Particle density
μ	Viscosity
λ	London's constant
ω_o	Constant used in equation 2.6.2
ε_o	Permeability of free space
υ	Volume

CHAPTER 1

INTRODUCTION

The normal approach to coal cleaning involves wet separation processes. When coal is cleaned in wet processing circuits, a waste stream containing fine coal particles is produced. Out of more than 1 billion tons of coal mined in the U.S. this year, only 350-400 million tons of useable clean coal was obtained. Very little attention has been paid to the coal fines since it is a very difficult process to enhance their quality. This was a very significant concern since the waste slurry would cause damage to the environment as well as resulting in the waste of precious coal resources. Since the dry separation process based on density difference has been a success at West Virginia University, the next step in this research would be to develop a system capable of separating fine coal particles from mineral matter, such as pyrite, which the larger circulating fluidized bed (CFB) is not capable of handling owing to its larger dimensions due to which it can only handle certain size ranges.

Therefore there was a need to design and test an experimental riser system which could process particles in the 0-150 micron size range. The three main goals of this study were the following.

1: To conduct exploratory investigation of separation of pyrite from fine coal in the riser.

2: To explore different injection techniques for injection of fine coal in the riser.

3: To determine the effect of iron particles on the separation of pyrite from coal.

Different feed mechanisms were used to test their performance for transport of fine particles in the riser. This system used the transition from fast fluidization to entrained flow within the riser. The air and coal mixture exhibited upward flow in the core of the riser while denser solids flowed downwards in the annulus along the pipe wall. These denser particles were collected in a collection bin. The low density particles passed through a series of cyclones and ended up in a collection bin. The very fine particles were captured in the filter.

A series of tests were run in order to evaluate the performance of the system. These tests were run at different mass fluxes and different air flow rates. The coal being tested in this system was chemically analyzed for sulphur content. The three streams of coal exiting the system, namely; out of the riser, out of the cyclone system and from the filter were also analyzed for the sulphur content. These results were evaluated for the different test conditions to evaluate the feasibility of this system to be used at coal preparation plants.

CHAPTER 2

BACKGROUND AND LITERATURE REVIEW

2.1 The Need of Fine Coal Handling System

In the past 20 years, wet processing plants have been the focus of the industry. One of the major factors that have effected the dry coal cleaning methods have been the dust generation, noise and vibration as well as the size range that can be introduced in the systems.

Currently the coal processing plants recover fine coal only from size fraction greater than 100 mesh (greater than 150 micrometers). This has been achieved using water only cyclones, spirals or combination of both for a size range of 16 x 100 mesh (1.0 millimeter to 150 micrometer) Buisman (2000).With no treatment, the fine coal usually smaller than 150 micrometers is sent to a thickener and then sent to a slurry impoundment. By employing a dry method for treating this fine coal, production of slurries can be reduced and even eliminated.

The pyritic sulphur, during combustion, produces sulphur dioxide (SO_2) which is a major pollutant in the environment. It combines with water vapors to form sulphuric acid (H_2SO_4) and produce acid rain. The reduction of pyritic sulphur in coal would help reduce pollution.

Section 2.2 gives a brief introduction to solid classification. Gas-solid fluidization, the terminal velocity of particles and fast fluidization regime

are covered in section 2.3, 2.4 and 2.5. Section 2.6 gives an introduction to the theory of van der Waals forces explaining the interparticle forces. Section 2.7 explains the previous research conducted on dry separation of particles in a riser based on density differences at West Virginia University. The purpose of covering these topics is to give the reader an insight of how fluidization occurs within a riser and how the size distribution of solids, the interparticle forces, and the terminal velocity of solids affects the dry separation process within the riser.

2.2 Particle Classification

Geldart (1972, 1973) introduced a useful classification scheme that classifies the solid particles into four broad groups; namely A, B, C and D. Powders belong in one of these four groups primarily depending on the mean diameter of particles and their density.

Figure 2.2.1 shows the different classes of solid particles.

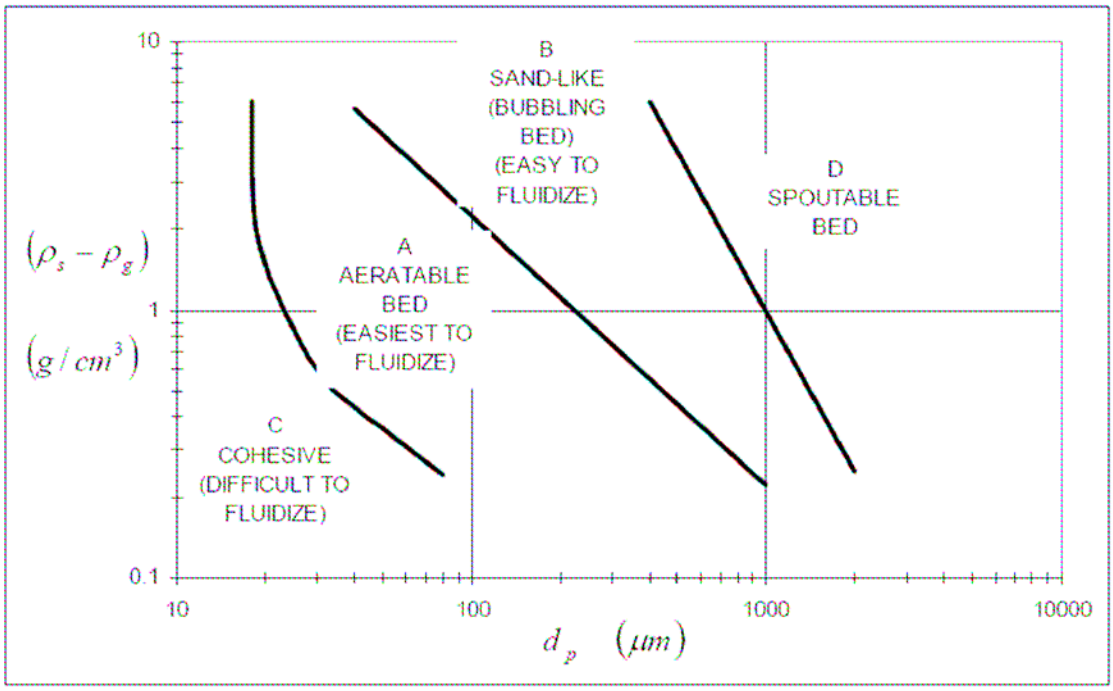

Figure 2.2.1 Different Classes of Solid Particles identified by Geldart (1972)

For the particle densities in this thesis, the diameter of particles in group C are below 20µm while for those in group A, are between 20 and 90 µm. A and C class particles are of interest in this study since the size range of solids used in this study is 0-150 micrometers.

The boundary between C and A class particles is not well defined and depends on the gas humidity, electrical properties (resistivity and dielectric constant) of the particles, density and mean diameter of the particles and on the gas properties. Very fine particles belong to group C and are difficult to fluidize. Starting at U_{mf} , group A particles enter a region of non bubbling fluidization followed by bubbling fluidization with increased gas velocity and eventually ending up in the region of fast

fluidization. A and C class particles are affected by the electrostatic forces as well as the interparticle forces.

For materials that are hard to fluidize i.e. group C particles, one or more of the following processes can be employed to induce minimum fluidization.

1: Vibration of the column either mechanically or by acoustic means.

2: Pulsation of the supply of fluidizing fluid.

3: Stirring or agitation of the contents of the vessel.

4: Addition of the fluidizing aid(like adding solids with larger diameter) to the powder.

2.3 Gas-Solid Fluidization

When a gas flows through a packed bed of particles, the pressure loss increases with an increase in the gas flow rate due to friction. As the gas flow rate is increased, a point is reached where the solid particles are supported by the drag exerted by the gas. The particles are then in a mobile condition and this condition is referred to as the onset of fluidization. Pressure drop for a bed of particles with density ρ_f and gas density ρ_g to form a bed of depth H and voidage ε is given by

$$\Delta p = H(1-\varepsilon)(\rho_p - \rho_f)g \qquad (2.3.1)$$

A plot of bed pressure drop versus the superficial gas velocity is shown in Figure 2.3.1.

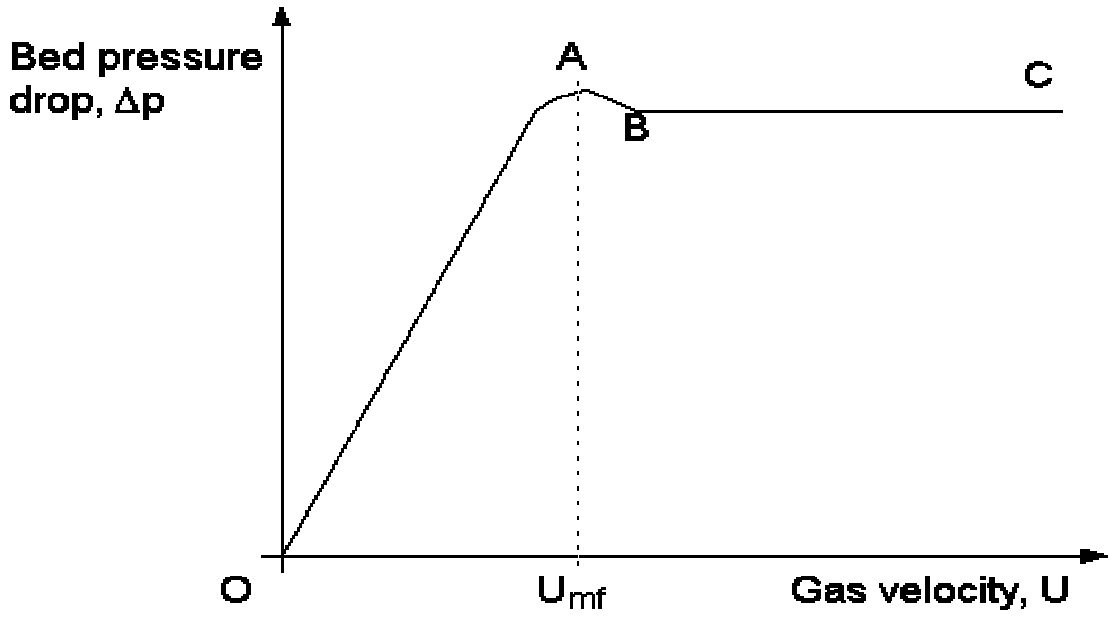

Figure 2.3.1 Bed pressure drop versus superficial velocity curve Rhodes (2001).

The region OA is the packed bed region where the separation between the particles is constant and they do not move relative to each other. The pressure loss versus the gas velocity in this region is given by the Ergun equation (1952).

$$\left(\frac{-\Delta p}{H}\right) = 150\frac{(1-\varepsilon)^2}{\varepsilon^3}\frac{\mu U}{d_s^2} + 1.75\frac{(1-\varepsilon)}{\varepsilon^3}\frac{\rho_f U^2}{d_s} \qquad (2.3.2)$$

At point A, pressure drop is higher than given by equation 2.3.1 showing that extra force is needed to overcome inter-particle attraction. The region BC is where equation 2.3.1 applies. Increasing the velocity beyond U_{mf} results in formation of bubbles for A class particles.

The minimum fluidization velocity U_{mf}, for particles greater than 100μm, was given by Wen and Yu (1966) correlation

$$\mathrm{Re}_{mf} = 33.7[(1 + 3.59 * 10^{-5} Ar)^{0.5} - 1] \qquad (2.3.3)$$

Where

$$\mathrm{Re}_{mf} = \frac{d_p U_{mf} \rho_f}{\mu} \qquad (2.3.4)$$

And

$$Ar = \frac{\rho_f (\rho_s - \rho_f) g {d_p}^3}{\mu^2} \qquad (2.3.5)$$

Minimum fluidization velocity for particles less than 100μm was given by the correlation of Baeyens (1974).

$$U_{mf} = \frac{(\rho_p - \rho_f)^{0.934} g^{0.934} {d_p}^{1.8}}{1110 \mu^{0.87} {\rho_g}^{0.066}} \qquad (2.3.6)$$

2.4 Terminal Velocity of Particles

An effective parameter for dry separation of solid particles in the riser is the terminal velocity of solid particles. Regester (2004) ran a mixture of sand and steel particles in a fluidized bed riser and found out that for gas velocities smaller than the terminal velocity of steel particles and higher than the terminal velocity of sand particles, effective separation of sand and steel particles occurred in the riser. According to Fan and Zhu (1998), terminal velocity of a spherical particle is related to its diameter by

$$U_{pt}^{1.4} = 0.072 \frac{d_p^{1.6}(\rho_p - \rho_g)g}{\rho_g^{0.4}\mu^{0.6}} \qquad 2<\mathrm{Re}_t<500 \qquad (2.4.1)$$

The Reynolds Number is given by

$$\mathrm{Re}_t = \frac{\rho U_{pt} d_p}{\mu} \qquad (2.4.2)$$

In this study, equation 2.4.1 was used to determine the terminal velocity of particles. This equation is accurate and was simple to use. It has been used in the previous West Virginia University study, Regester (2004).

2.5 Fast Fluidization Regime

A fast fluidization regime has been described, Yerushalmi (1976), as a dense, entrained suspension characterized by an aggregative state in which much of the solid is segregated in large and densely packed clusters.

The lower bound for the gas velocity, Fan and Zhu (1998), for the fast fluidization regime (U_{tf}) is given by

$$U_{tf} = 39.8\sqrt{gdp}\left(\frac{G_p}{\rho U_{tf}}\right)^{0.311} \mathrm{Re}_t^{-0.078} \qquad (2.5.1)$$

where G_p is the mass flux of solids into the system.

The upper bound for the gas velocity, Fan and Zhu (1998), for the fast fluidization regime (U_{fd}) is given by

$$U_{fd} = 21.6\sqrt{gd_p}\left(\frac{G_p}{\rho U_{fd}}\right)^{0.542} Ar^{0.105} \qquad (2.5.2)$$

where

$$Ar = \frac{\rho(\rho_p - \rho)gd_p^{\,3}}{\mu^2} \qquad (2.5.3)$$

Equation 2.5.1 and 2.5.2 can be applied to group A particles in small diameter risers (D<0.2m). All observed radial distribution profiles of particle velocity support the core-annulus flow structure where solids are mainly entrained upwards in the core region and descend in the annular region, Lim, Zhu, Grace (1995). Yang (1995) observed the solid behavior and determined particle velocities in the annulus region close to the wall and the interface of the core-annulus region. Figure 2.5.1 shows the velocity profile in a riser of a circulating fluidized bed. The abscissa was shown as the ratio of the thickness of the annulus region to the radius of the riser. From the experiments, it was concluded that the core-annulus flow interface moved away from the wall as the superficial velocity was decreased as well as the increase in the solid mass flux.

Lim, Zhu and Grace (1995) proposed four types of particle flow structures along the wall of a riser.

1: Particle clusters: Groups of particles congregated in the riser to reduce the effective drag force exerted on them.

2: Particle streamers: Dense bands larger than the size of the clusters observed in the core region and along the walls of circulating fluidized beds.

3: Particle swarms: Dense particle assemblies at the wall when a riser is operated under relatively dilute conditions.

4: Particle sheets: Two dimensional layers of densely populated particles near the bed wall.

2.6 van der Waals Forces

There are different types of adhesion forces that exist between solid particles. These include mechanical, chemical, dispersive, electrostatic and diffusive adhesion. van der Waals force is a type of dispersive adhesion that holds the opposite charges of two molecules together. In group C powders, cohesive behavior can be explained due to interaction of particles under van der Waals forces. These forces cause the powder to adhere to the processing equipment and also result in the clogging of pipes. Agglomeration may be due to van der Waals forces and cause solid settling. When fluidizing the C particles, these forces are dominant and

result in non homogenous fluidization. This results in formation of cracks and channels in the bed.

2.6.1 Background

In 1873, van der Waals explained the non ideal behavior of gases by concluding that this behavior is due to atomic interactions. His famous equation of state is given by

$$(P + \frac{n^2 a}{V^2})(V - nb) = nRT \qquad (2.6.1)$$

where *b* accounted for the finite volume occupied by the gas molecules and *a* was related to the strength of the intermolecular forces.

2.6.2 Theory and Developments

In 1936, London explained the dispersion effect concluding that the dispersion effect is a result of the Van der Waals forces. The dispersion effect is the interaction between instantaneous dipoles of atoms due to the motion of orbiting electrons. London's equation is given by

$$E = -\frac{3}{4}\hbar\omega_0\left(\frac{R_0}{R}\right)^6$$

where

$$\omega_0 = \frac{2\left(\frac{e}{m_e^{0.5}}\right)}{\left(\frac{\alpha_A^{\,0}}{N_A}\right)^{0.5} + \left(\frac{\alpha_B^{\,0}}{N_B}\right)^{0.5}} \qquad (2.6.2)$$

and

$$R_0^{\,6} = \frac{\alpha_A^{\,0}\alpha_B^{\,0}}{(4\pi\varepsilon_0)^2}$$

where α is the zero frequency polarizability of a molecule, N is the number of electrons in the outer orbital of an atom, and ε is the permeability of free space. The changing dipole of one atom produces an oscillating electric field which acts on the neighboring atoms.

The polarizability of a molecule is its ability to respond to an external electric field by adjusting its own dipole i.e. changing the orientation of its own electrons so as to have a favorable orientation in the electric field. If the atoms are in vacuum, the induced dipole of the neighboring atom is in phase with the original dipole and attractive force occurs. This is given by

$$E = -\frac{\lambda_{i,j}}{H^6} \qquad (2.6.3)$$

where λ is the London's constant and depends on the atomic numbers of the two atoms.

This force is attractive in dilute gas phase. This equation is valid only for distances less than the wavelength of the major electronic adsorption band for the gas. If the distance is greater than this, retardation comes into play. Retardation is caused by the fact that if the atomic separation is large, the electric field generated by the oscillating atom has to travel further and the induced dipole of the neighboring atom becomes out of phase with the original dipole since the original dipole is also changing its orientation. Now the following equation is obtained.

$$E = -\frac{23\hbar c \alpha_A^{\,0} \alpha_B^{\,0}}{4\pi(4\pi\varepsilon_0)^2 R^7} \qquad (2.6.4)$$

This force becomes inversely proportional to R^7.

In 1937, Hamaker used the microscopic theory of Van der Waals forces i.e. the concept of additivity and found out that the non retarded energy of interaction is given by

$$E = -\int_{v_1} dv_1 \int_{v_2} dv_2 \frac{q_1 q_2 \lambda_{1,2}}{H^6} \qquad (2.6.5)$$

van der Waals force is given by

$$F = \frac{\partial E}{\partial H} \qquad (2.6.6)$$

van der Waals forces have been calculated using equation 2.6.6 for different solid geometries. For example in the case of two spheres of radius *a* and *b*, van der Waals force is given by

$$F = -\frac{A}{6H}\left(\frac{ab}{a+b}\right) \qquad (2.6.7)$$

where A is the Hamaker's constant and is given by

$$A = \pi^2 q_1 q_2 \lambda_{1,2} \qquad (2.6.8)$$

In 1956, Lifshitz introduced the modern theory of van der Waals forces. The fundamental idea is that the interaction between two bodies is propagated in the form of electromagnetic waves and these waves are analyzed using Maxwell's equations. The medium between the two bodies is treated as a continuum and its bulk properties introduced through permeability. The macroscopic approach depends on the idea of correlated fluctuations i.e. the motion of electrons around one atom is affected by the motion of electrons around its surrounding atoms and even those further away. The macroscopic body can be considered of consisting of many oscillating dipoles and therefore continuously radiate energy and also absorb energy from the electromagnetic field generated by the surrounding atoms.

Most of this energy stays inside the body and results in its cohesive energy. The electromagnetic energy that escapes the body is contained in the surface vibrational modes of the body. The electromagnetic absorption spectrum of the body determines what frequencies of the electromagnetic energy can the body absorb and to what extent it can absorb them.

The free energy per unit area for two half spaces made up of materials 1 and 2 and separated by a distance H filed with a gas or vacuum is given in terms of the surface modes of reciprocal length κ.

$$E_{1,2} = \frac{kT}{2\pi} \sum_{n=0}^{\infty'} \int_0^{\infty} [\ln(1 - \Delta_{1,n}\Delta_{2,n} e^{-2\kappa H})] \kappa d\kappa \qquad (2.6.9)$$

where

$$\Delta_{j,n} = \frac{\varepsilon_j\{\iota\varepsilon_n\} - 1.0}{\varepsilon_j\{\iota\varepsilon_n\} + 1.0} \qquad (2.6.10)$$

and

$$\varepsilon_n = n[\frac{2\pi kT}{h/2\pi}] \text{ n= 0, 1, 2....} \qquad (2.6.11)$$

where T= absolute temperature, k= Boltzman's constant and h= Plank's constant. In the above equation, ε_n is nth thermal fluctuation mode. The prime on the summation sign shows that n=0 is given half weight. The

quantity $\varepsilon_j\{i\xi_n\}$ is related to the complex dielectric permeability which is the electrical response of the bulk material to an external electric field and is related to the polarizability of the constituent atoms.

$$\varepsilon\{\omega\} = \eta^2\{\omega\}$$
$$\eta^2\{\omega\} = 1.0 + \frac{C_{UV}}{1.0 - \{\frac{\omega}{\omega_{UV}}\}^2} \qquad (2.6.12)$$

In equation 2.6.12, C_{uv} and ω_{uv} are the oscillator strength and frequency of the principal ultraviolet absorption peak. In this study, literature was studied for adhesive forces that might exist between iron and pyrite atoms. A theoretical study of this force was found but no practical approach was found for calculating the magnitude of van der Waals force between iron and pyrite particles.

2.7 Previous Research at WVU

The earlier research in West Virginia University (Johnson, Kang, and Regester) focused on separation of particles based on density differences. The test mixtures consisted of two different materials namely sand and steel shots. This concept of separation in a riser of a CFB was established and it was observed that the separation took place in the transition region between fast fluidization regime and dilute regime. Different exit geometries for the riser were tested. The effects of internal rings and the collection gaps on the separation process were studied. The experimental

results showed that changing the collection gap width had no effect on the separation process in the riser. Heavy particle collection efficiency improved with the increase in height of the riser. An internal ring ratio of 0.8 was shown to increase the dense particle mass fraction in the collection bin at high flow rates. It was noted that at low mass fluxes, the separation process was successful and more than 90 % of the dense particles were collected in the dense particle collection bin.

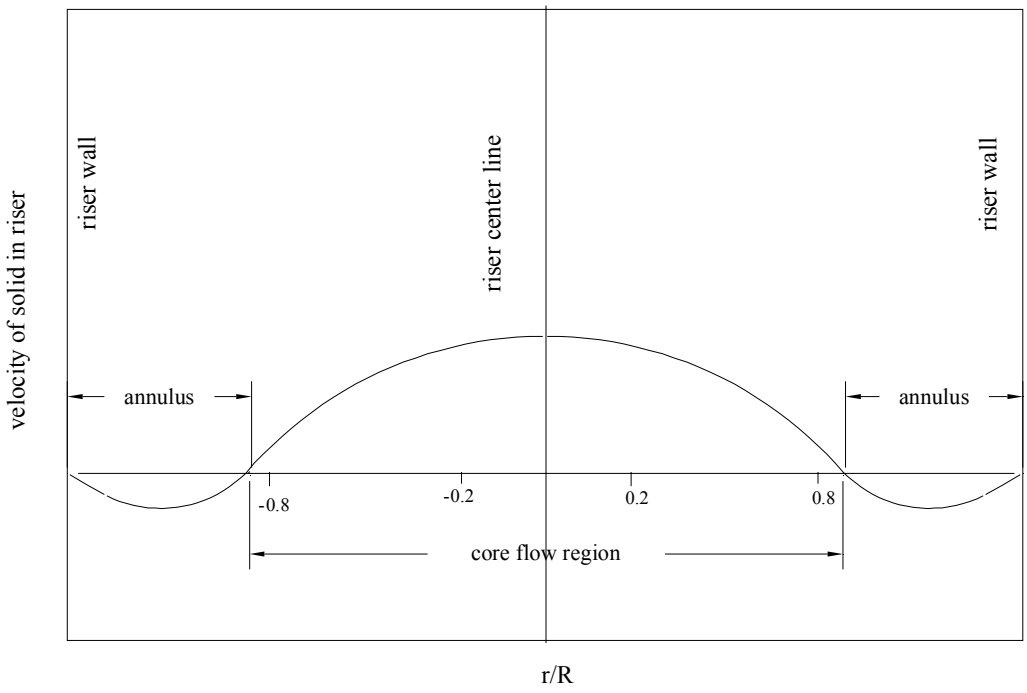

Figure 2.5.1 Velocity Profile in a riser of a CFB (Yang 1995).

CHAPTER 3

EXPERIMENTAL SYSTEM

3.1 Fluidized Bed Riser System

A fluidized bed riser system was designed to study separation of coal particles from pyrite in the size range of 0-150 micrometers. This system was built in the High Bay area of NRCCE. It consisted of an acrylic riser, acrylic feed hopper as well as a two stage cyclone system as shown in Figure 3.1. Solids were fed from the hopper into the riser pneumatically. Downstream of the riser, the cyclones delivered particles to the product hoppers and very fine particles were collected in the filter downstream of the cyclones. The effects of different mass fluxes and superficial velocities on the separation of pyrite from coal were to be studied in this system. Different feeder mechanisms for the introduction of solids into the riser were built and tested. The concern was the problem with the injector previously encountered with particles smaller than 100 micrometer in diameter. Testing was also to be performed using a mixture of pure iron and coal to observe the effect of presence of iron on the separation of pyrite from coal. The complete system is shown in Figure 3.1.

3.2 Design of the Riser

The riser was made from a clear acrylic tube with an inside diameter of 2 inches and an outside diameter of 2.5 inches. The ends of the riser were attached to flanges made out of acrylic sheets 0.5 inches thick. The flanges were attached with the acrylic tube using acrylic adhesive and steel pins 1/32 inches in diameter. The riser was 6 feet high with a side exit port. A 0.5 inch thick acrylic cap was connected to the top flange of the riser. The flange was bolted by six ¼ inch threaded bolts. A paper gasket was introduced between the flange and the cap ensuring that there was no air leak. A 90 degree ¾ inch PVC elbow was connected to the exit port at the top of the riser for solid exit. The bottom of the riser was connected by flanges with the distributor plate housing made from acrylic tube. Six bolts were used to hold the flanges in place with a paper gasket used to seal the joint. The gasket helps to avoid any air leaks. For additional strength, the flanges were sealed from the outside using adhesives. The L/D ratio for this riser was 36 while the L/D ratio for the riser of the larger fluidized bed system was 33.6. The riser is shown in Figure 3.2.

3.3 Design of the Distributor Plate

The distributor plate is one of the major components of the fluidized bed system. The distributor plate was machined from a 1 3/4 inch stainless steel 303 solid rod. It was designed in the shape of a funnel at 60 degrees

with a ½ inch opening at the bottom. It was held in place with two ½ inch steel pipes with one end threaded. Air was introduced in one of these pipes while the other pipe was sealed at the end. The distributor plate was placed in an acrylic tube with a 2 inch inner diameter. There was a 1/8 inch gap between the distributor plate and the inner walls of the acrylic tube. This gap was introduced so as to allow the dense solid particles to flow past the distributor plate and end up in the collection bin. The distributor plate is shown in Figure 3.3.

3.4 Cyclone Design

A two stage cyclone system was designed to ensure maximum separation of solids from gas. Both the cyclones were designed according to the instructions found on page 92 of Air Pollution Engineering Manual, Danielson (1967). Both the cyclones were 2 inches in diameter and are shown in Figure 3.4.a. The purpose of the second cyclone was to remove any dust in the air stream after the first cyclone. The two cyclone approach also allowed for two product streams. As the results showed, the cyclones may also act to separate pyrite from coal particles.

The flow rates through the cyclones were in the range of 7.5 to 12.5 SCFM. Inlet velocity V_i was calculated by dividing the flow rate by the inlet area.

Total pressure drop across a cyclone is given by

$$P_{total} = V_i^2 \rho_g \frac{\Delta H}{2}$$

where ρ_g is the gas density. ΔH is given by

$$\Delta H = 16 \frac{H_c B_c}{D_e^2}$$

The cyclone cut off size is the diameter of the particles in which the cyclone should have a collection efficiency of 50% and is given by

$$D_{pc} = \sqrt{\frac{9\mu B_c}{2NV_i \rho_p \pi}}$$

where N is the number of turns that the solids make in the cyclone. The following table shows the performance characteristics of the cyclones.

Table 3.4 Cyclone Design Parameters

Operating Condition	1	2
Design Parameters	7.5 SCFM	12.5 SCFM
Flow rate (m^3/s)	0.0035	0.0059
Area (m^2)	0.0005	0.0005
Inlet Velocity (m/sec)	7	11.8
Total Pressure Drop (N/ m^2)	505.7	1436.9
Number of turns	3	3
Cut off size (Micrometers)	4.52	3.48

3.5 Solid Injection Design

Solid particles were pneumatically injected into the riser using either feeder configuration A, B and C. Feed configuration A is shown in Figure 3.5.a. Feed configurations B and C are discussed in detail in section 4.3. Feed configuration A consisted of two air inlets. The first air inlet was on top of the feed hopper pushing the solid particles down. The second air inlet was at the elbow of the PVC pipe conveying the solids to the riser. This air inlet helped reduce the built up of fine coal in the horizontal pipe thus eliminating problems regarding clogging of the horizontal pipe due to fine solid particles. Consequently, configuration A was used for the separation test runs.

3.6 Hopper Design

The hopper was made out of clear acrylic tube with a 5 inch inner diameter and 5 ½ inch outer diameter. It was flanged on the top end with an acrylic flange ½ inch thick and was capped off on the top with a clear acrylic cap ½ inch thick. This cap was bolted with the flange using six ¼ in bolts around the circumference of the flange. A pressure gauge was connected to the hopper in order to monitor the pressure in the hopper. Solids were introduced from the top through a ¾ inch opening in the cap and the hopper was open at the injector end. During the test, this opening in the cap was sealed with a steel bolt. The bottom of the hopper was

connected to the injection system via a rubber hose connector. This connector was clamped around the hopper using hose clamps.

3.7 Collection Bins

There were three collection locations for the solid particles in the system. These were called the dense bin and the two product bins. Dense particle collection bin for the dense particles was made from acrylic tube with a 2 inch inner diameter. It had a flange at one end with six ¼ inch steel bolts. This top part was connected to the distributor plate housing. The bottom part was capped off with acrylic sheet which was ½ inches thick. Two ¾ inch diameter PVC pipes were employed as the product bins with ¾ inch PVC ball valves for the solid stream coming out of the two cyclones. The solids in these two product bins were mixed together.

3.8 Filters

For the very fine solid particles, vacuum cleaner filters were used to trap the fine particles. A ¾ inch PVC pipe, with holes 1/16 inch in diameter drilled around the pipe, carries the fine particles into the filter as shown in Figure 3.6. The purpose of the holes drilled around the pipe is to ensure continuous air flow rate and eliminate any pressure built up in the filters. Hoover type H filter bags were used in the system.

3.9 Instrumentation

This experimental system was connected with two air flow meters. The two flow meters were the Omega FLMG series in-line pneumatic flow meters. The flow meters were rated at a pressure of 100 psi at 100 SCFM. These meters measured the air flow rate into the pneumatic injection system and the distributor plate. The air flow rate was converted into superficial velocity by dividing it by the cross sectional area of the riser. There were two pressure gauges 2 feet apart in the riser and one pressure gauge in the hopper. The hopper was suspended by a load cell which gave a read out of the solid flow rate in the system. The load cell was Omega LC101-200 with a maximum load capacity of 200 pounds. The load cell was attached to the frame using an S hook made from stainless steel. The mass flow rate was converted into mass flux by dividing it by the cross sectional area of the riser. The load cell was connected with the data acquisition board DAP 5200a/526 mounted in the computer. DAP View was used to read the signal and convert it into appropriate units. The load cell was calibrated using known weights of three, five and ten pounds.

3.10 System Limitations

The goal of this thesis was to build a small scale system with a very minimum of funding to study the separation of fine particles. Therefore this system was built to do exploratory work at a minimum expense. A series of tests were conducted to determine the operating limits of the system. It was observed that increasing the solid mass flux more than 5 kg/m^2-sec for superficial velocity of 3 m/s resulted in coal dust leaking around the hopper as well as around the PVC elbow joints. Increasing the superficial velocity more than 3 m/s resulted in rupturing of the filter bags. It was observed that the injector system took longer to inject solids into the riser for low air flow rates (e.g. it took the injector 45 minutes to inject 2 pounds of solids into the riser for an air flow rate of 7.5 SCFM and a solid mass flux of 1.1 kg/m^2-sec).

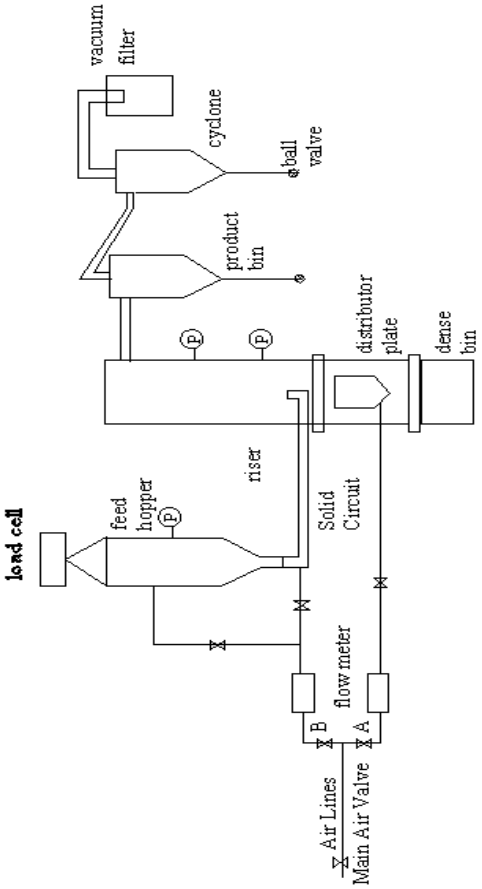

Figure 3.1 System Layout

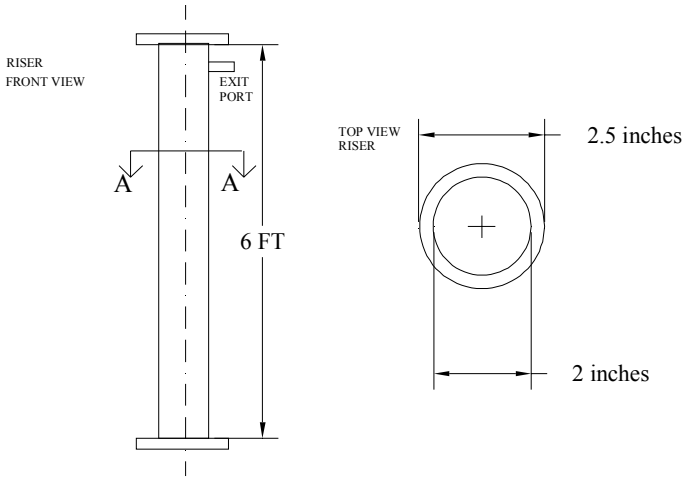

Figure 3.2 Riser

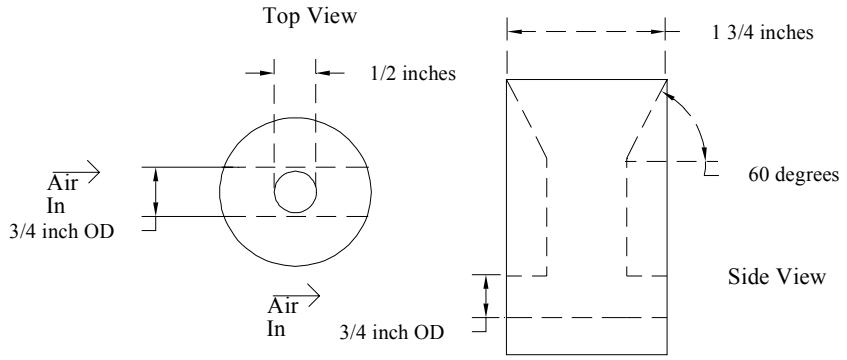

Figure 3.3 Distributor Plate

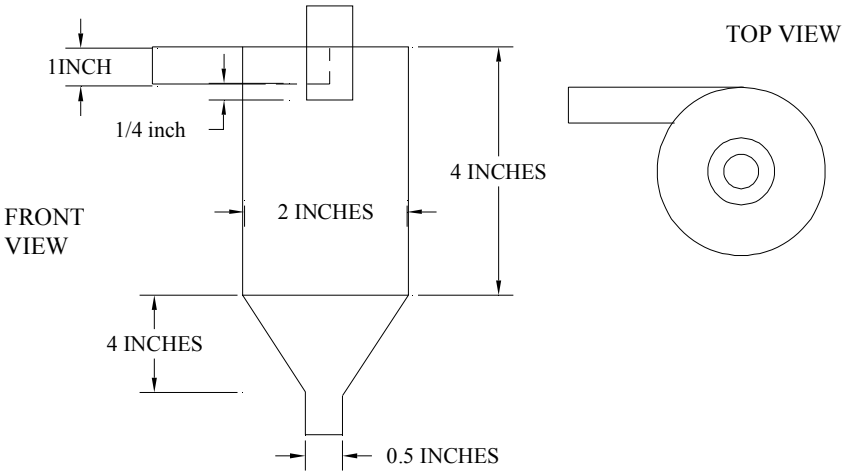

Figure 3.4.a. Cyclone Dimensions

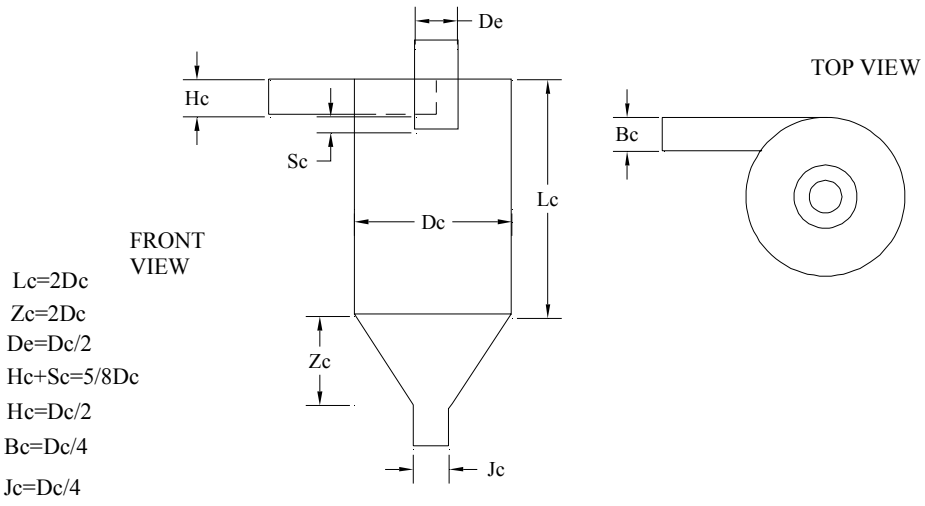

Figure 3.4.b. Cyclone Design Terminology

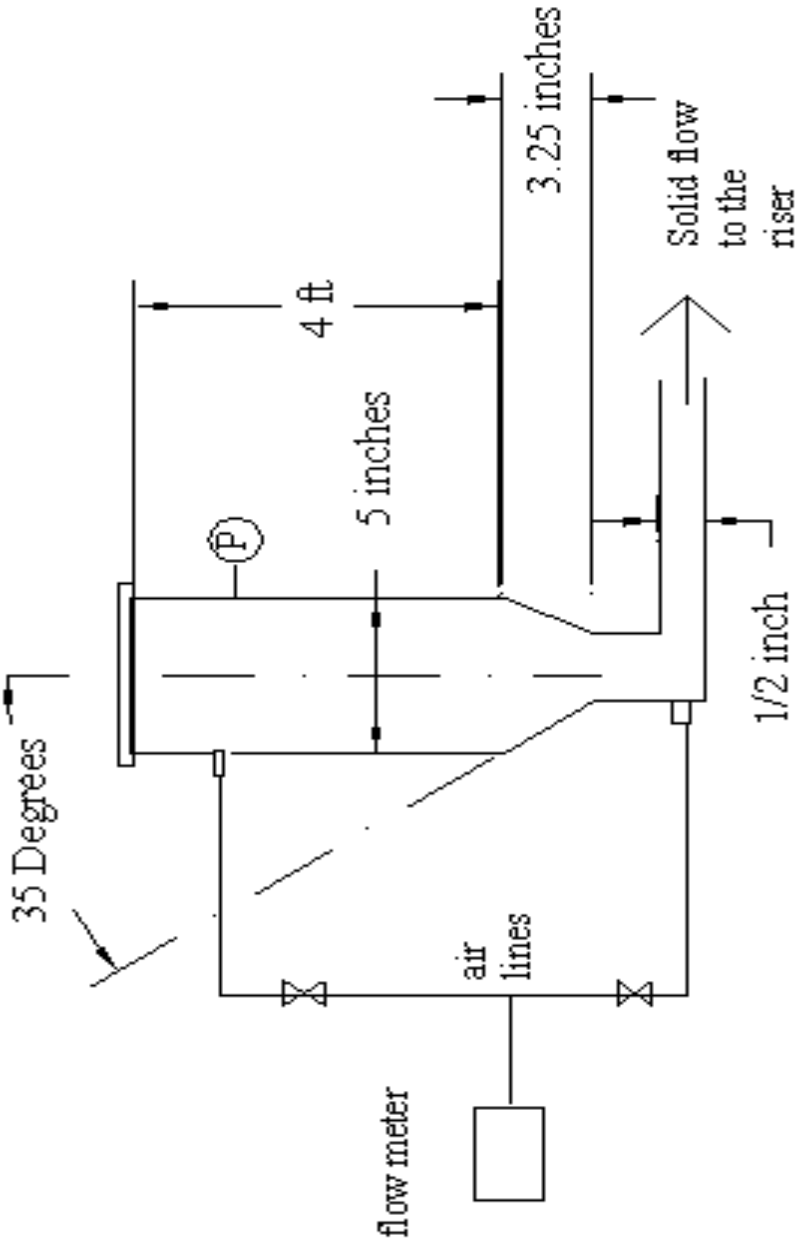

Figure 3.5 Feed Configuration A

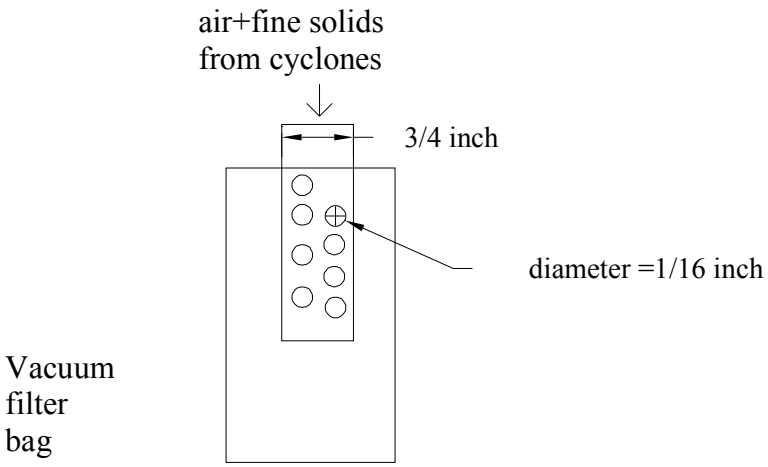

Figure 3.6 Filter

CHAPTER 4

SYSTEM PERFORMANCE AND TESTING

4.1 Experimental Procedures

The testing was performed on the system in the High Bay area of NRCCE. Compressed air was supplied from Sulair compressor at a pressure rating of 110 psi. Primary source for air supply within the system was the distributor plate while the secondary supply was the pneumatic solid injection system.

4.1.1 Start-up Procedure

The following steps were taken during start up of the system for each test.

1. Sample is taken from the coal prior to the test and sent to the chemical analysis lab to determine the sulphur content.
2. Turn on the output meters for load cell reading.
3. Make sure that all the air supply valves are off.
4. Turn on the PC and log on to DAPView.
5. Introduce the pre-weighed coal into the feed hopper.
6. Seal the feed hopper.
7. Attach the pre-weighed filter bag to the filter outlet.
8. Close the ball valves sealing the exit under the cyclones to collect the fine coal particles.
9. Turn on the main air supply valve on

10. Turn on the air supply valve A to the distributor plate to the desired level.
11. Turn on the air supply valve B to the solid injection system to the desired level.
12. Adjust the air flow rates till the selected value and steady state is achieved.

4.1.2 Experimental Observations

During the course of the test, the following observations were made.

1. The data was saved for the solid flow rate from DAPView.
2. Pressure gauges were monitored to insure that the pressure in the system does not exceed 1.5 psi.
3. Air flow rate was noted from the flow meters.
4. Visual observation was made to determine and note the flow regime within the riser.

4.1.3 Shut-down Procedure

The following steps were taken at the end of each test.

1. Air supply valve B to the pneumatic solid injection was turned off.
2. Air supply valve A to the distributor plate was turned off.
3. Main air supply valve was shut down.
4. Data in the computer was saved for the test readings.
5. Dense bin was removed from the system and the dense particles were weighed.

6. Ball valves were opened and the solids from the product bin were combined and weighed.
7. Filter was removed from the system and weighed.
8. Samples were taken from the coal in the dense, product and filter bin.
9. Computer is turned off and the samples are sent to the lab for elemental analysis.

4.1.4 Test Matrix

As it was discussed earlier, when the solid mass flux was increased more than 5 kg/m^2-sec, it resulted in dust leaks from the flanges in the system. Increasing the air flow rate past 12.5 SCFM resulted in rupturing of the filter bags. This established the upper limit of the system with regards to the solid mass flux and the air flow rate. The superficial velocities and the corresponding solid mass fluxes were selected to be in the transition region from fast fluidization to dilute regime. This was done because Regester's work (2004) showed that the most effective separation of solids based on density difference took place in the riser in the transition region from fast fluidization to dilute regime. Therefore a test matrix was designed keeping the above mentioned conditions in consideration. Section 4.5 gives more detail about the size distribution of Consol coal used in these tests. The size range of the iron particles was 0-150 micrometer. Size of the coal sample in the test runs was 5 pounds. The run time for tests depended on the total air flow rate supplied to the

system. For 7.5 SCFM, it was approximately 30 minutes while for 12.5 SCFM, it was approximately 15 minutes.

Table 4.1.4 Test Matrix

Superficial Velocity (m/s) Air Flow Rate (SCFM)	Range of Solid Mass Flux (Kg/m^2-sec)
1.5 m/s 7.5 SCFM	1-2.75
2.5 m/s 10 SCFM	1.25-3
3 m/s 12.5 SCFM	1.75-3.5

4.2 **Cyclone Performance**

Cyclone efficiency is defined by the following equation.

$$\eta_{cyclone} = \frac{\text{mass in the product bin}}{\text{mass approaching the cyclone}}$$

The cyclone efficiency is shown in Figure 4.2.a and 4.2.b. Increasing the superficial velocity decreased the efficiency of the cyclone for the actual test runs as shown in Figure 4.2.a. The efficiency of the cyclone improved as the superficial velocity was increased for the coal-iron mixture as shown in Figure 4.2.b. In both cases, an increase in the solid

mass flux resulted in a decrease in cyclone efficiency. One data point (G=3.3 kg/m^2-s, U_o=1.5 m/s, η= 74%) was outlying as shown in Figure 4.2.b for no obvious reason. Figure 4.7 shows the inlet gas velocity in a cyclone vs. pressure drop across a cyclone. Pressure drop increases with an increase in inlet gas velocity.

4.3 Solid Injection Performance

In this system, solid particles were injected into the riser using a pneumatic injection system consisting of a non mechanical L valve. In some experimental systems, fine solid particles are injected in the riser using a screw feeder (Banhart, Knuwer). However that was an additional expense raising the cost and maintenance expense of the system making it more complicated. Therefore three feeder configurations and two injection designs were tested and analyzed. It was found that the injection process worked the best when the air injector was placed in the elbow of the L valve. This design was called injector A, as shown in Figure 4.3.a. In design C, the air injector was placed at two diameter length above the elbow as shown in Figure 4.3.a. Design C did not work well and solid particles started clogging the horizontal pipe and steady state could not be achieved.

The solid stream was independent of the air injection in the distributor plate. The pipe carrying the solids into the riser was six inches in length and a half inch in diameter. The solids were introduced into the

riser through a half inch elbow located inside the riser. In feed configuration A and C, no air was recirculated to the feed hopper. Feed configuration A used injector A and feed configuration C used injector C. A third feeder configuration known as feed configuration B was also tested where the air coming out of the primary cyclone was recirculated back to the feed hopper to reduce the pressure built up in the hopper. Feed configuration B used injector C. However steady state was hard to achieve in this configuration as well. It was found that in order to pneumatically inject solids in the riser, there had to be a certain threshold of solid mass in the feed hopper for the three feeder configurations. This ensured that the solids were injected continuously in the riser and steady state was achieved. Figure 4.3 shows the results of the three configurations for a total air flow rate of 12.5 SCFM. Out of this total air flow rate, 5 SCFM was supplied to the three feeder configurations. It can be seen that the steady state is achieved while using feed configuration A. The following empirical equation was obtained for feed configuration A.

$$m = -0.1766\ t + 2.0295$$

where m is the mass in the hopper in pounds and t is the time in minutes. In the 18 test runs, feed configuration A was used for injecting solids in the riser. The angle of friction in the hopper was 35 degrees and the angle of repose was 37 degrees for fine coal, Sud (2002).

4.3. a Mathematical Model of Feed Configuration

Hydrodynamic model proposed by Li (2003) for an L-valve has been modified for the feed configuration A and the modified results are described below.

First, vertical stand pipe had been considered and the vertical force acting at the bottom of the stand pipe was developed to be

$$Fy = \frac{4G^2}{\rho_p(1-\varepsilon_v)\pi D_1^{\,2}} + \frac{\pi D_1^{\,3}}{16 H_v D_c \mu_1} * \left[\rho_p(1-\varepsilon_v)g - \frac{p^* - p_2}{L_v} \right] \qquad (4.3.a.1)$$

The vertical stress at the bottom of the standpipe was

$$\sigma_y = \frac{D_1}{4 H_v D_c \mu_1} \left[\rho_p(1-\varepsilon_v)g - \frac{p^* - p_2}{L_v} \right] \qquad (4.3.a.2)$$

H_v is the ratio of the stresses near the vertical wall and D_c is the stress distribution factor for cylindrical moving bed (Li, 2003).

The gas velocity in the stand pipe was given by

$$u_{fy} = \frac{p^* - p_2}{L_v K_v} - \frac{4G}{\pi D_1^{\,2} \rho_p (1-\varepsilon_v)} \qquad (4.3.a.3)$$

where

$$K_v = 154 \left(\frac{1-\varepsilon_v}{\varepsilon_v} \right)^2 \frac{\mu}{dp^2} \qquad (4.3.a.4)$$

Flow rate of gas in the standpipe was given by

$$Qv = \frac{\pi}{4} D_1^{\,2} \varepsilon_v u_{fy} \qquad (4.3.a.5)$$

Horizontal contacting stress among particles at the entrance of the horizontal pipe was given by

$$(\sigma_x)_0 = \frac{4Fy\sin\theta_r(\cos\theta_r - \frac{8\mu_1}{3\pi}\sin\theta_r)}{\pi D_h{}^2} \qquad (4.3.a.6)$$

where μ_1 is the wall friction coefficient.

Pressure drop across the horizontal pipe was given by

$$\Delta P_h = p^* - p_1 = 4.266(\frac{d_p}{D_h})^{0.25} u_{sx}{}^{0.45} \rho_p(1-\varepsilon_h) g L_h - (\sigma_x)_0 \qquad (4.3.a.7)$$

where u_{sx} was the particle velocity given by

$$u_{sx} = \frac{G}{\rho_p(1-\varepsilon_h)\frac{\pi}{4}D_h{}^2} \qquad (4.3.a.8)$$

Average gas velocity in the horizontal pipe was given by

$$u_{fx} = \frac{p^* - p_1}{L_h K_h} + \frac{4G}{\rho_p(1-\varepsilon_h)\pi D_h{}^2} \qquad (4.3.a.9)$$

where K_h was given by

$$K_h = 154(\frac{1-\varepsilon_h}{\varepsilon_h})^2 \frac{\mu}{d_p{}^2} \qquad (4.3.a.10)$$

Gas flow rate in the horizontal section was given by

$$Q_h = \frac{\pi}{4} D_h{}^2 \varepsilon_h u_{fx} \qquad (4.3.a.11)$$

Aeration gas flow rate was given by

$$Q_L = Q_h - Q_v \qquad (4.3.a.12)$$

These sets of equations describe the complexity of the processes occurring in a feed configuration. In order to design and analyze an injector using these equations, a computer program would be required.

4.4Flow Regime in the Riser

The flow of the air and solid particles inside the riser was in the transition region from fast fluidization to dilute flow. Solids were injected in the riser six inches above the distributor plate. Core-annulus flow was observed in the riser with particle swarms descending along the wall with a dilute region observed at the top of the riser during the testing. Increasing superficial gas velocity or reducing solid mass flux resulted in reduction of the size and frequency of the appearance of the swarms. It was determined through visual observation that the dense particles ended up in the dense bin while the remaining solids were carried out by air through the exit port into the cyclones. Figure 4.4 shows the different flow regimes in the riser where the upper bound and the lower bound for the fast fluidization regime are given by equations 2.5.1 and 2.5.2.

4.5 Sieving Analysis

A coal sample is collected and then is passed through the screening process. At that time, for coal, the following screens were employed.

+60 mesh (+0.25 mm), 60-100 mesh (0.25-0.150 mm), 100-140 mesh (0.150-0.105mm), 140-200 mesh (0.105-0.074 mm), -200 mesh (-.074 mm).

These screens were the small screens with an 8 inch diameter that were available in the crushing room in the Mineral Resources Building. They could hold a maximum initial mass of ten pounds. In the screening process, conservation of mass principle is applied.

$\sum m$ (screen sizes) = $m_{initial}$

The coal samples were screened and data was recorded for five screening tests. The distribution of coal particles along the size distribution aforementioned is shown in Figure 4.5.

4.6 Error Analysis

Error analysis was performed to determine the error in the following readings.

1: Flow meters

2: Load cell

3: Sieve analysis

4: Chemical lab results

In the sieve analysis, 6 lbs of coal was put in the sieves and at the end, 5.7 lbs was collected. The error came out to be 5%. In the second run, 7 lbs of coal was loaded on the sieves and at the end of the run, 6.5 lbs of

coal was obtained. The error came out to be 7%. The error was due to the dust created by the sieving process.

In the chemical lab results, the standard deviation from the average value for each sample is listed in the lab reports and is listed in the appendix. Three samples were obtained from the material collected at each port. Each sample was tested three times for elemental analysis and standard deviation for each test and the average value of the three tests was reported. Standard deviation gave a measure of the deviation of each test value from the average value of the three tests. From the data, it can be seen that the value of standard deviation for the elemental analysis was less than 0.2 which means that the three test values were in excellent agreement with each other.

For the load cell error analysis, 15 pounds of solids were loaded in the hopper and the output meter displayed 15.3 lbs giving an error of 2%. When the hopper was loaded with 25 pounds of solids, the output meter displayed 25.4 pounds giving an error of 1.6%. The load cell has a linearity factor of $\pm$ 0.03% and repeatability factor of $\pm$ 0.01%.

The flow meters have a measuring accuracy factor of $\pm$ 2.5 % of full scale in the center third of the measuring range. In this case, this range is from 5 SCFM to 12.5 SCFM. The repeatability factor for these flow meters is $\pm$ 1%.

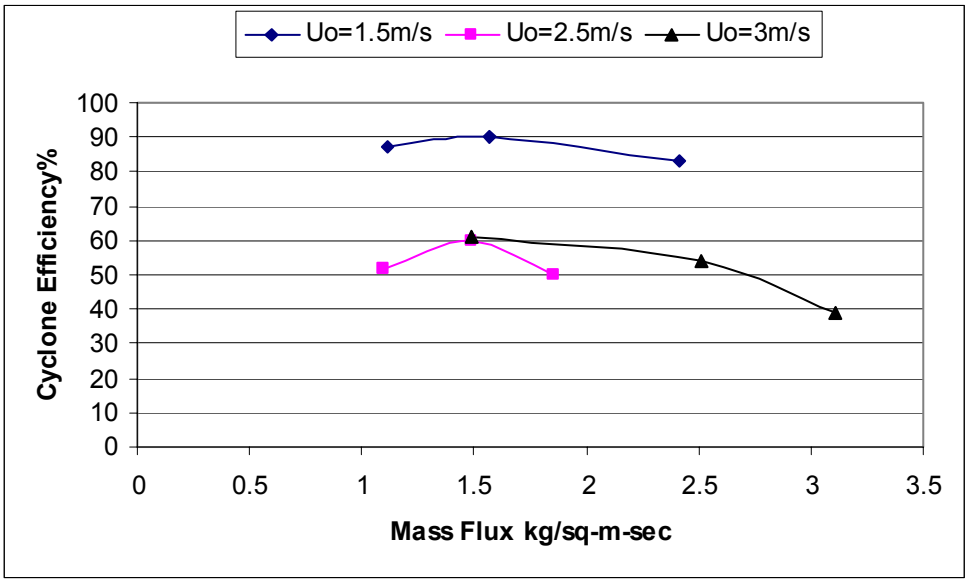

Figure 4.2.a. Cyclone efficiency for coal tests

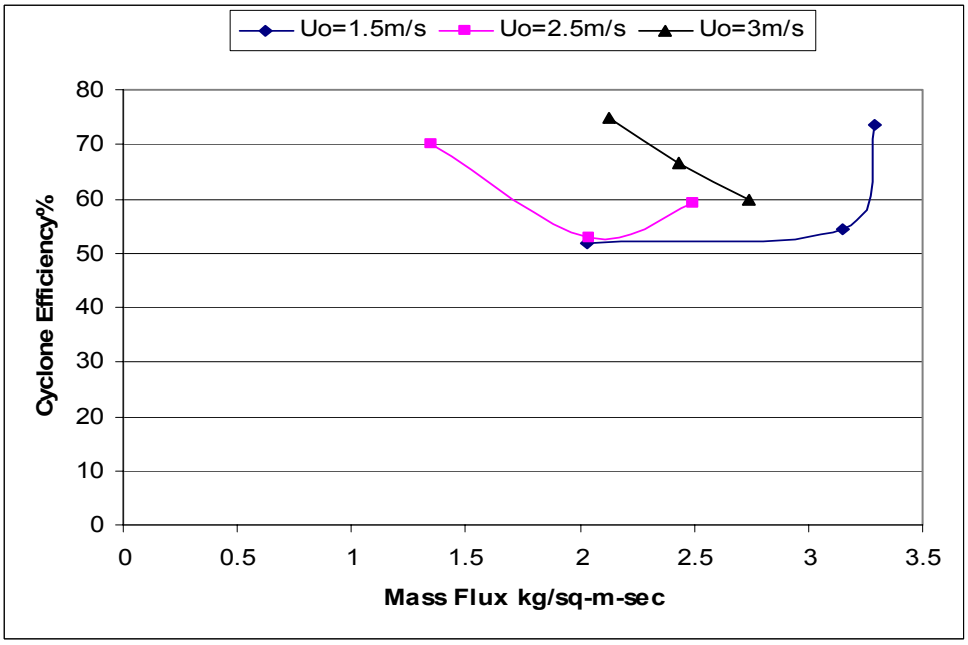

Figure 4.2.b. Cyclone efficiency for coal/iron tests

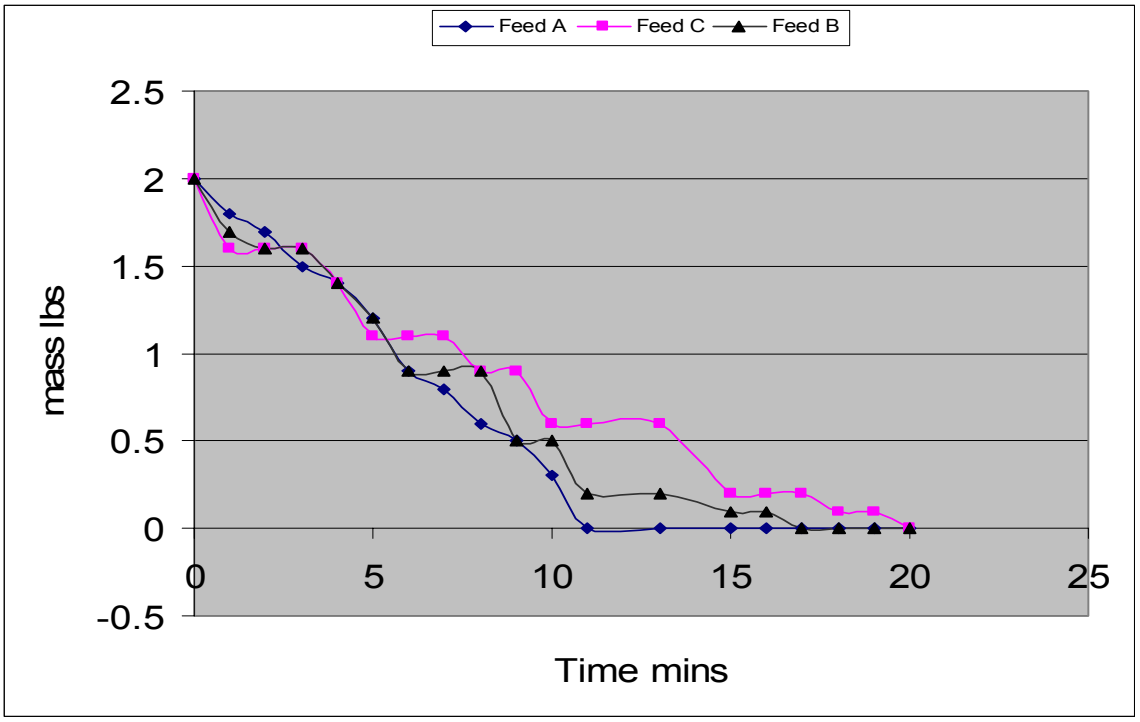

Figure 4.3 Feed Configuration Comparison, mass in the hopper as a function of time. Test conditions (Air flow rate of 5 SCFM to the feeder configuration, total air flow rate =12.5 SCFM to the riser and Uo = 3 m/s in the riser).

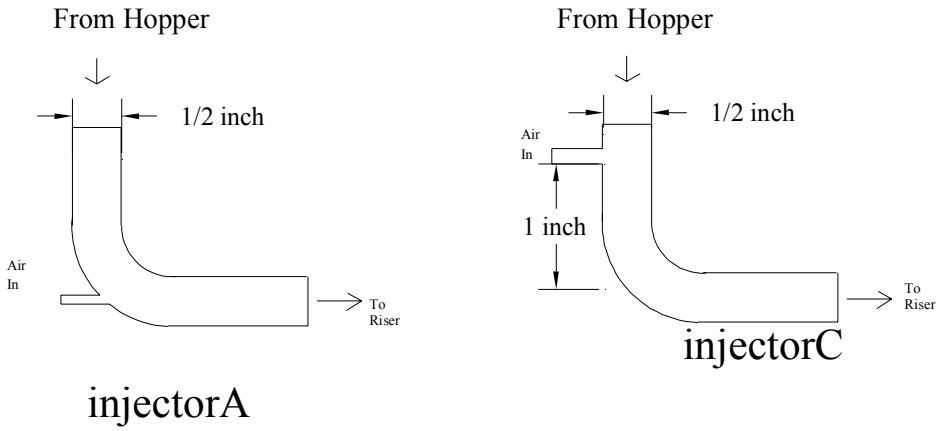

Figure 4.3.a Injectors

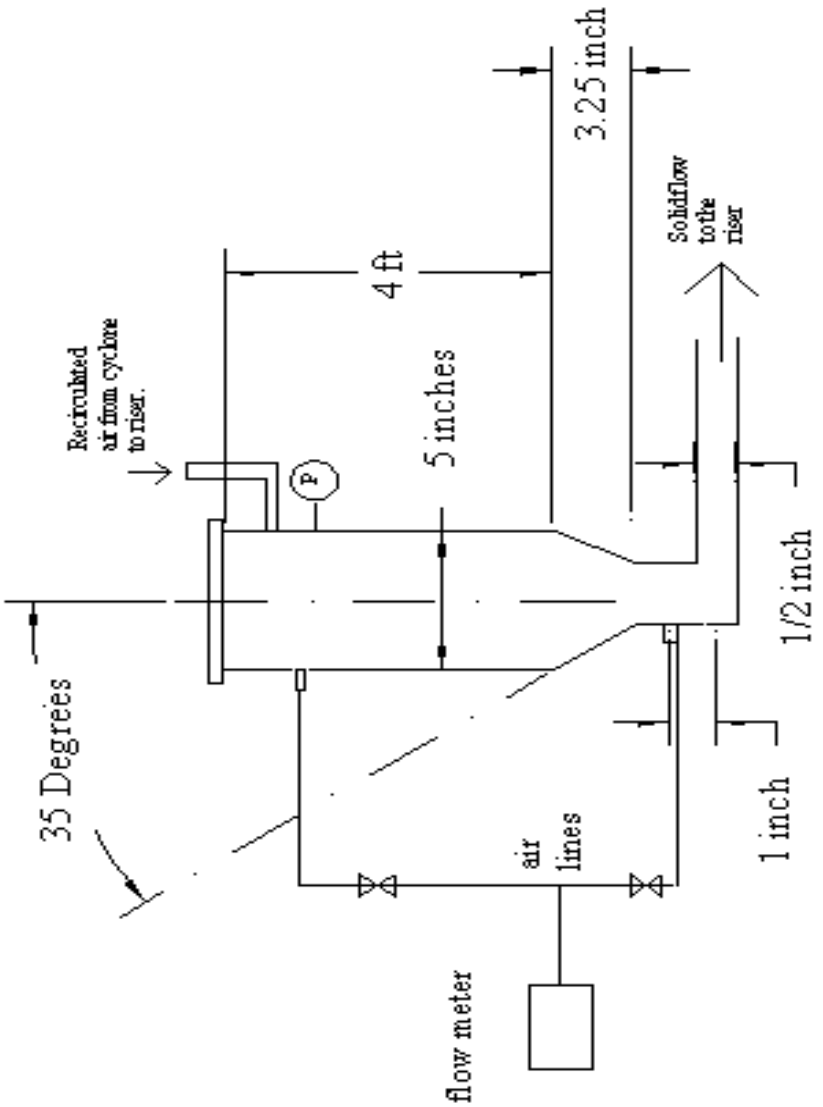

Figure 4.3.b. Feed Configuration B

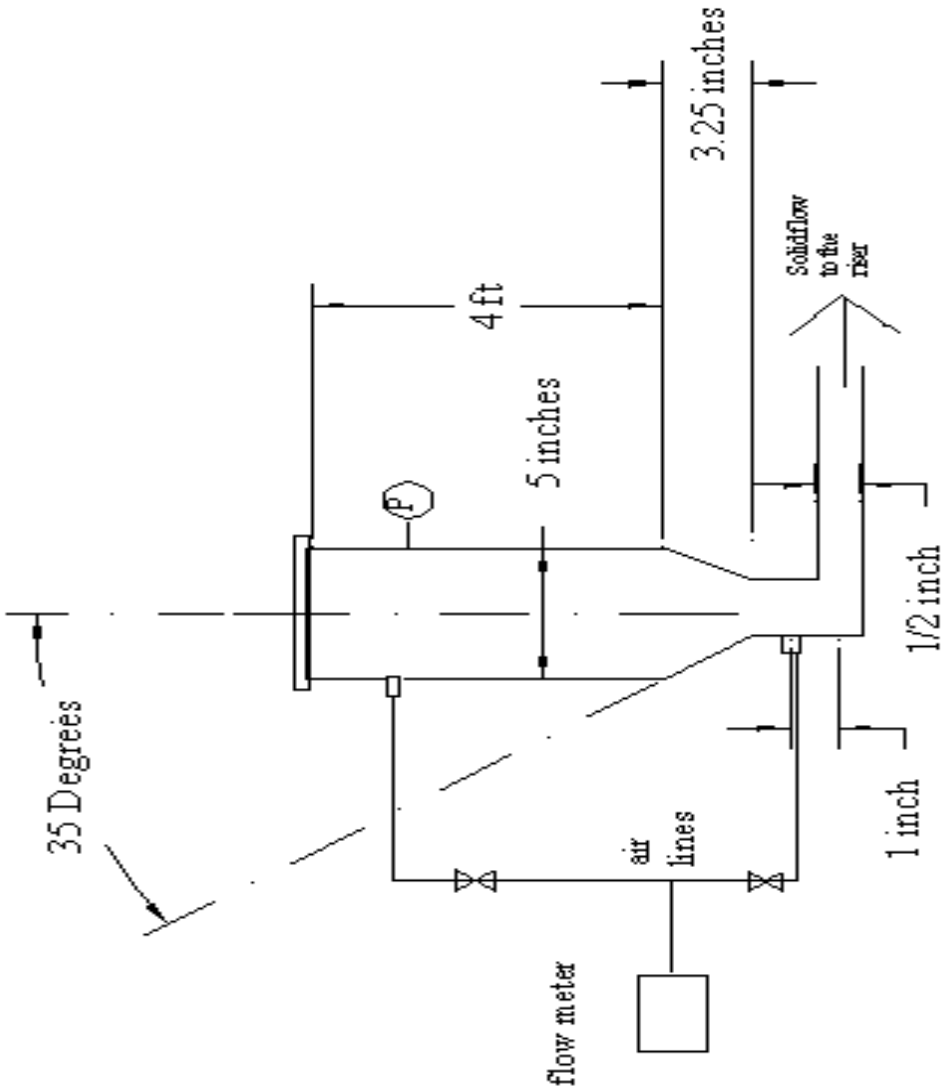

Figure 4.3.c Feed Configuration C

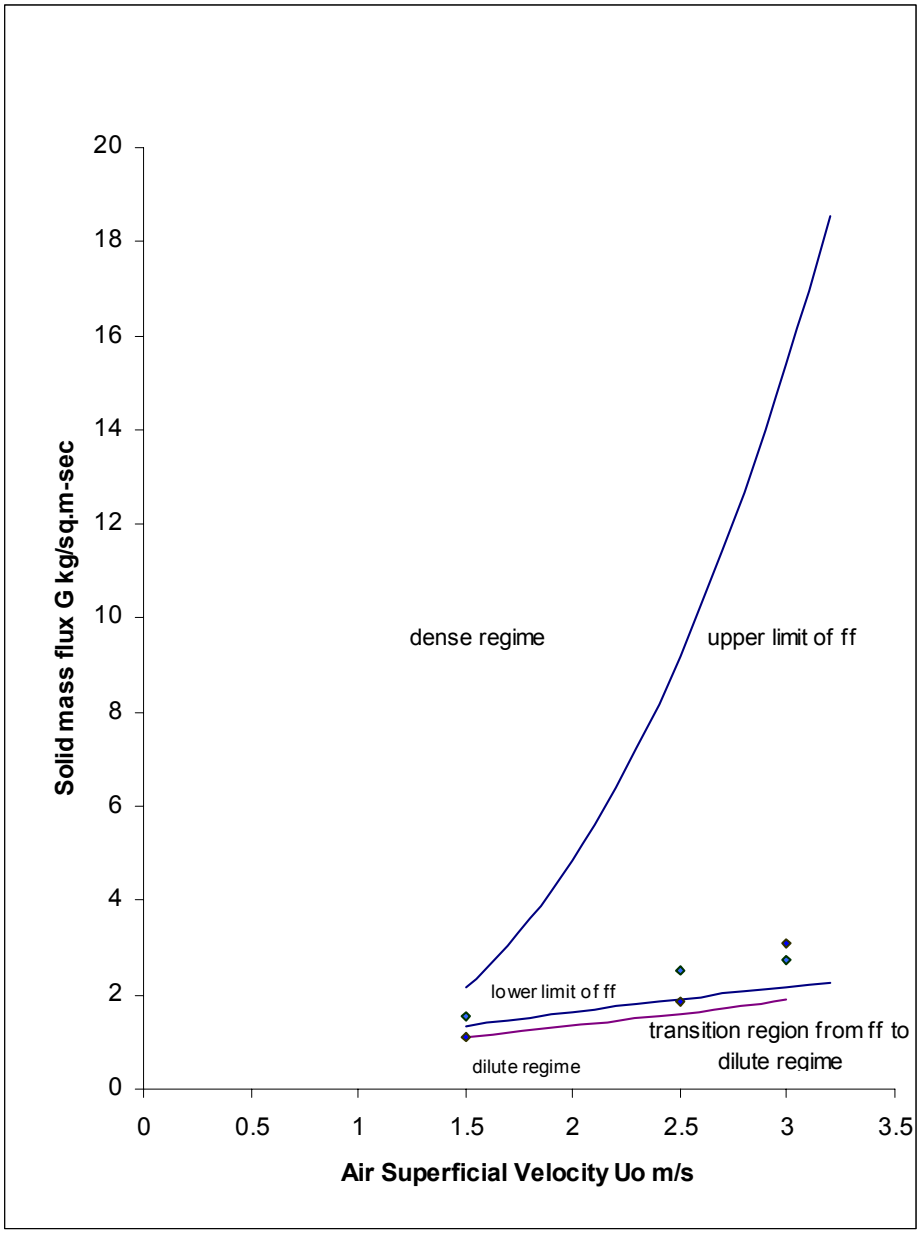

Figure 4.4 Experimental Flow Regime in the Riser

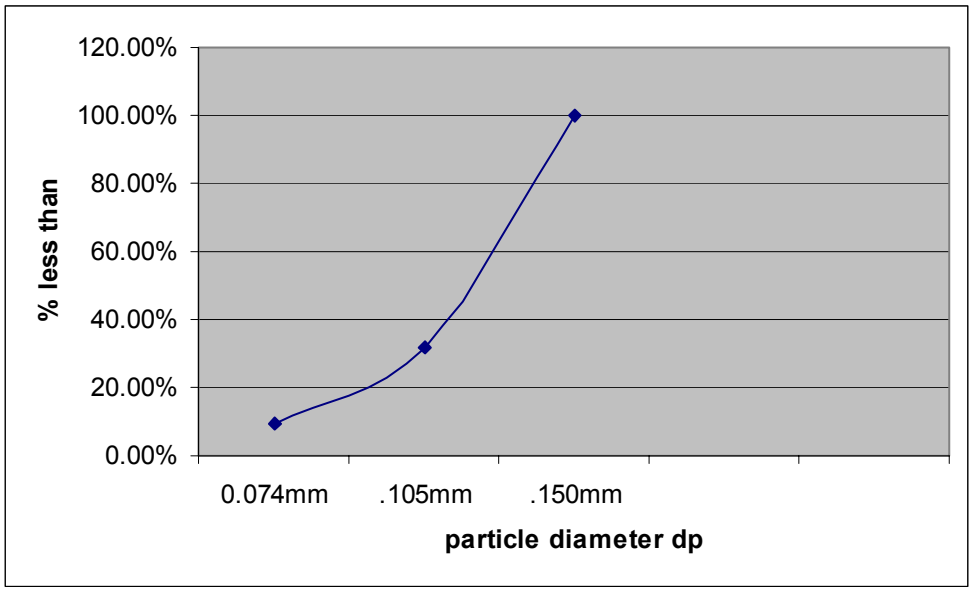

Figure 4.5 Size Distribution of Consol Coal

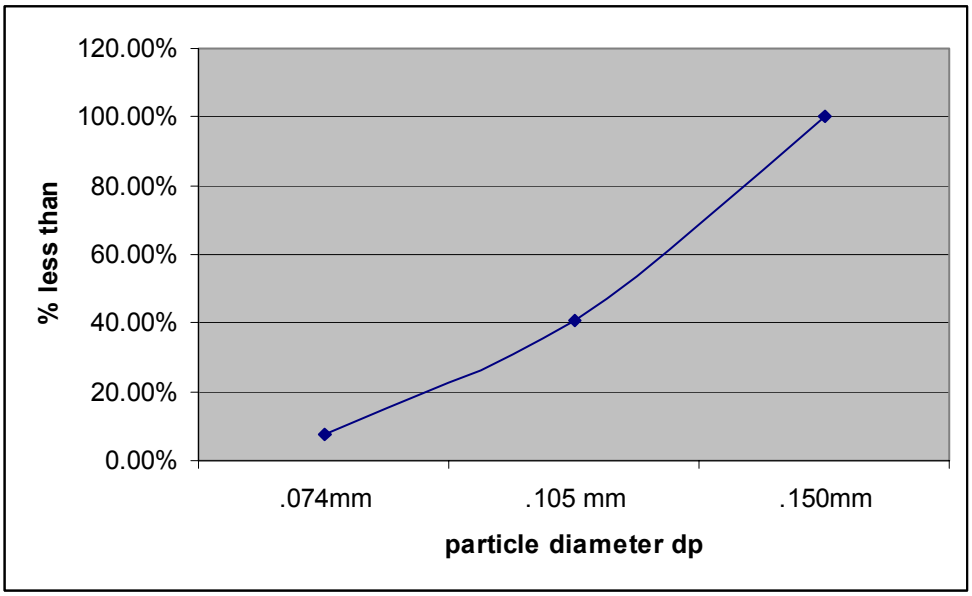

Figure 4.6 Size Distribution of Iron

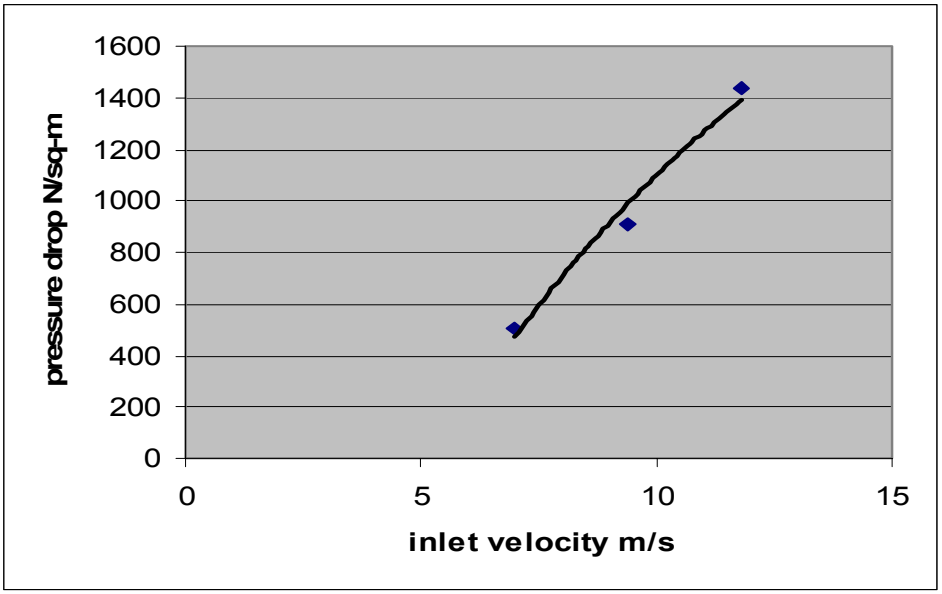

Figure 4.7 Pressure Drop across a Cyclone

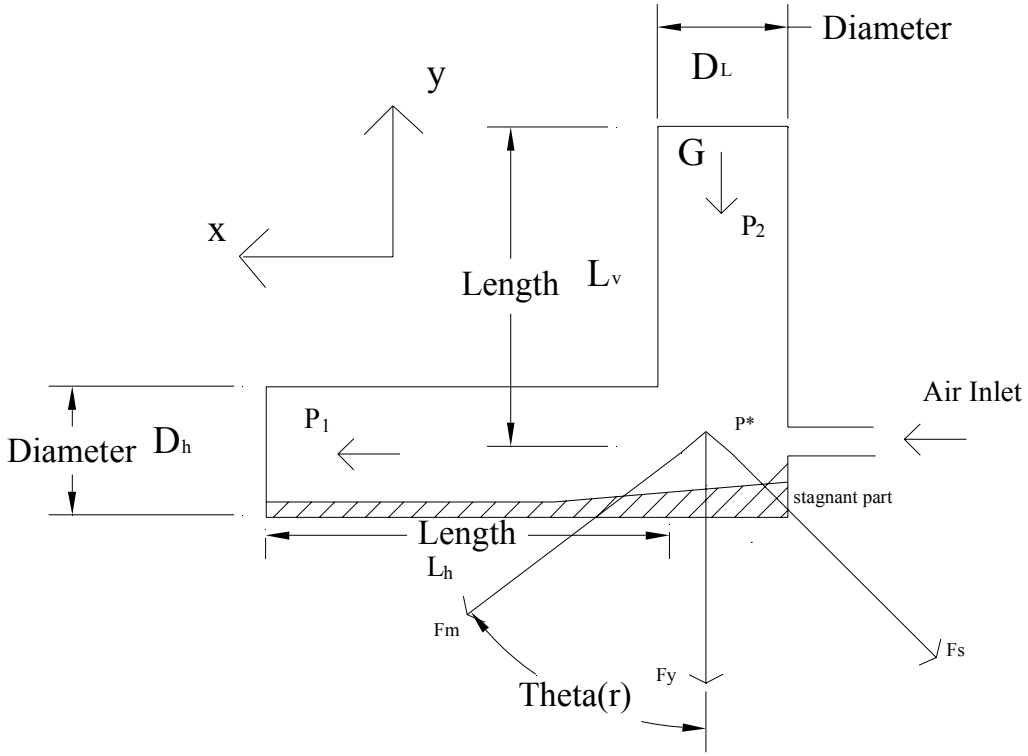

Figure 4.8 Injector A Math Model

CHAPTER 5

RESULTS

A series of tests were run using feed configuration A in the system to observe the separation process at different superficial velocities and different solid fluxes. A total of nine tests were run using 100% coal while nine tests were run using a mixture of 10% iron and 90% coal by mass. This testing had no effect on ash and the ash content remained uniform at each exit port.

5.1 Coal Test Results

Nine tests were run using three different superficial velocities for coal. The results are summarized in the table below are based on a 100 lb sample.

Table 5.1

Sulphur Analysis for Coal (100 lb pretest mixture)

Test #		Pretest Sulphur	Dense bin sulphur	Product bin sulphur	Filter sulphur
4 –coal Uo=2.5m/s G=1.4858 kg/m^2-s	Ms(lb) Ms(Kg) % S %mass collected	2.55 lbs 1.16 kg	0.7 lbs 0.32 kg 2.8 25	1.2 lbs 0.54 kg 2.7 45	0.65 lbs 0.29 kg 2.4 27.5
5 -coal Uo=2.5 m/s G=1.0982 kg/m^2-s	Ms(lb) Ms(Kg) % S %mass collected	2.75 lbs 1.25 kg	0.65 lbs 0.29 kg 2.9 22.5	1.25 lbs 0.57 kg 3.1 40	0.95 lbs 0.43 kg 2.7 35
6- coal Uo=2.5 m/s G= 1.8544 kg/m^2-s	Ms(lb) Ms(Kg) % S %mass collected	2.55 lbs 1.16 kg	0.55 lbs 0.25 kg 2.7 20	1.05 lbs 0.48 kg 2.6 40	1.05 lbs 0.48 kg 2.8 38

10 –coal Uo= 3 m/s G= 1.4858 kg/m^2-s	Ms(lb) Ms(Kg) % S %mass collected	2.75 lbs 1.25 kg	0.3 lbs 0.14 kg 3 10	1.8 lbs 0.82 kg 3.3 55	0.85 lbs 0.39 kg 2.6 32
11 –coal Uo= 3 m/s G=2.5118 kg/m^2-s	Ms(lb) Ms(Kg) % S %mass collected	2.75 lbs 1.25 kg	0.25 lbs 0.11 kg 3.3 7.5	1.55 lbs 0.7 kg 3.1 50	1.2 lbs 0.54 kg 2.9 40.5
12 –coal Uo= 3m/s G= 3.1046 kg/m^2-s	Ms(lb) Ms(Kg) % S %mass collected	2.75 lbs 1.25 kg	0.35 lbs 0.16 kg 3.5 10	1.2 lbs 0.54 kg 3.4 35	1.55 lbs 0.7 kg 2.9 54
13 –coal Uo= 1.5 m/s G=1.1096 kg/m^2-s	Ms(lb) Ms(Kg) % S %mass collected	3.45 lbs 1.56 kg	1.25 lbs 0.57 kg 3.1 40	1.85 lbs 0.84 kg 3.5 52.5	0.15 lbs 0.07 kg 3 5
14 –coal Uo=1.5 m/s G=1.5656 kg/m^2-s	Ms(lb) Ms(Kg) % S %mass collected	3.05 lbs 1.38 kg	1.7 lbs 0.77 kg 3.4 50	1.35 lbs 0.61 kg 3 45	0.05 lbs 0.02 kg 1.7 3
15 –coal Uo= 1.5 m/s G= 2.4168 kg/m^2-s	Ms(lb) Ms(Kg) % S %mass collected	3.05 lbs 1.38 kg	1.85 lbs 0.84 kg 3.4 55	1.1 lbs 0.5 kg 2.9 37.5	0.1 lbs 0.04 kg 1.7 6

From the data, it can be seen that the filter bin has the least amount of sulphur content as shown in Figure.5.3a and 5.3.b. In test 14 run at a superficial velocity of 1.5 m/s, 3% of the solids were collected in the filter with a sulphur content of 1.7%. In test 4 run at a superficial velocity of 2.5m/s, 27.5% of the total coal ended up in the filter bin with a sulphur content of 2.4%. For superficial velocity of 3m/s, no separation of coal from pyrite was observed and small mass was collected in dense bin. This was because the air velocity was high compared to the terminal velocity

of the solid particles and most of the solid particles were carried out of the riser by the air.

5.2 Coal/Iron Mixture Results

Nine tests were conducted with superficial velocities of 1.5 m/s, 2.5 m/s and 3 m/s. In these tests, 10% iron by mass was added to the coal. The iron was added to observe the effect of iron particles on the separation of pyrite from coal. The following table summarizes the results.

Table 5.2

Sulphur Analysis for 100 lb Coal/Iron mixture

Test #		Pretest	Dense Bin	Product Bin	Filter
7 coal+ 10% Fe Uo=2.5 m/s G=2.0406 kg/m^2-s	Ms(lb) Ms(Kg) % S %mass collected	2.55 lbs 1.16 kg	0.35 lbs 0.16 kg 2.3 15	1.25 lbs 0.57 kg 2.8 45	0.85 lbs 0.39 kg 2.4 36
8 coal+ 10% Fe Uo=2.5 m/s G=2.4966 kg/m^2-s	Ms(lb) Ms(Kg) % S %mass	2.55 lbs 1.16 kg	0.4 lbs 0.18 kg 2 20	0.9 lbs 0.41 kg 1.9 47.5	0.65 lbs 0.29 kg 2.1 30.5
9 coal+ 10% Fe Uo=2.5 m/s G=1.3528 kg/m^2-s	Ms(lb) Ms(Kg) % S %mass collected	2.55 lbs 1.16 kg	0.65 lbs 0.29 kg 2.6 25	1.2 lbs 0.54 kg 2.3 52.5	0.045 lbs 0.02 kg 2.1 21.5
16 coal+ 10% Fe Uo= 1.5 m/s G=3.1502 kg/m^2-s	Ms(lb) Ms(Kg) % S %mass	3.45 lbs 1.56 kg	1.7 lbs 0.77 kg 3.8 45	1.05 lbs 0.48 kg 3.5 30	0.65 lbs 0.29 kg 2.95 22
17 coal+ 10% Fe Uo= 1.5 m/s G=3.2946 kg/m^2-s	Ms(lb) Ms(Kg) % S %mass collected	3.05 lbs 1.38 kg	1.8 lbs 0.82 kg 3.4 52.5	1.1 lbs 0.5 kg 3.1 35	0.25 lbs 0.11 kg 2.3 11
18 coal+ 10% Fe Uo= 1.5 m/s G=2.0254 kg/m^2-s	Ms(lb) Ms(Kg) % S %mass collected	2.75 lbs 1.25 kg	1.25 lbs 0.57 kg 3.3 37.5	0.9 lbs 0.41 kg 2.8 32.5	0.6 lbs 0.27 kg 2.2 27
19 coal+ 10% Fe Uo= 3 m/s G=2.1318 kg/m^2-s	Ms(lb) Ms(Kg) % S %mass	2.55 lbs 1.16 kg	0.6 lbs 0.27 kg 3 20	1.55 lbs 0.7 kg 2.6 60	0.45 lbs 0.2 kg 2.4 19
20 coal+ 10% Fe Uo= 3 m/s G= 2.432 kg/m^2-s	Ms(lb) Ms(Kg) % S %mass collected	2.55 lbs 1.16 kg	0.45 lbs 0.21 kg 2.6 17.5	1.4 lbs 0.63 kg 2.5 55	0.55 lbs 0.25 kg 2.1 25.5
21 coal+ 10% Fe Uo= 3 m/s G= 2.7436 kg/m^2-s	Ms(lb) Ms(Kg) % S %mass	2.55 lbs 1.16 kg	0.4 lbs 0.18 kg 3.2 12.5	1.3 lbs 0.59 kg 2.5 52.5	0.7 lbs 0.32 kg 2.2 32

It can be seen that in case of coal/iron mixture, the filter bin has the least sulphur content for all three superficial velocities. In test 21, run at a superficial velocity of 3 m/s, 32 % of the solids ended up in the filter bin with a sulphur content of 2.2%. In test 8 run at a superficial velocity of 2.5m/s, 30.5% of the total solids ended up in the filter with a sulphur content of 2.1%. As opposed to pure coal test mixtures, use of coal/iron test mixtures for superficial velocity of 3m/s resulted in separation of coal from pyrite. However low amount of solids were collected in dense bin. This was because the air velocity was high as compared to the terminal velocity of the solid particles and most of the solid particles were carried out of the riser by the air.

5.3 Separation of Coal from Pyrite

In these tests, there has been an insignificant separation of pyrite from coal. The Filter bin had a percentage of sulphur lower than the percentage of sulphur in the sample introduced into the system for 13 test runs. Figure 5.3.e shows the percentage of sulphur in initial sample, the dense bin, the product bin and the filter for test 4. Figure 5.3.e shows that the coal collected in the filter in test 4 had the lowest sulphur content. Figure 5.3.f shows that 27.5% of the initial sample was collected in the filter in test 4. Figure 5.3.g shows that the coal collected in the filter in test 16 had the lowest sulphur content. Figure 5.3.h shows that 22% of the initial sample was collected in the filter in test 16. Consequently the potential

for the separation appears to exist with the cyclone as a separation mechanism. The results relative to the filter bag collection were the basis for concluding that the coal collected in the filter had the lowest sulphur content. Figure 5.3.a shows a plot of percentage sulphur content in the filter for various mass fluxes.

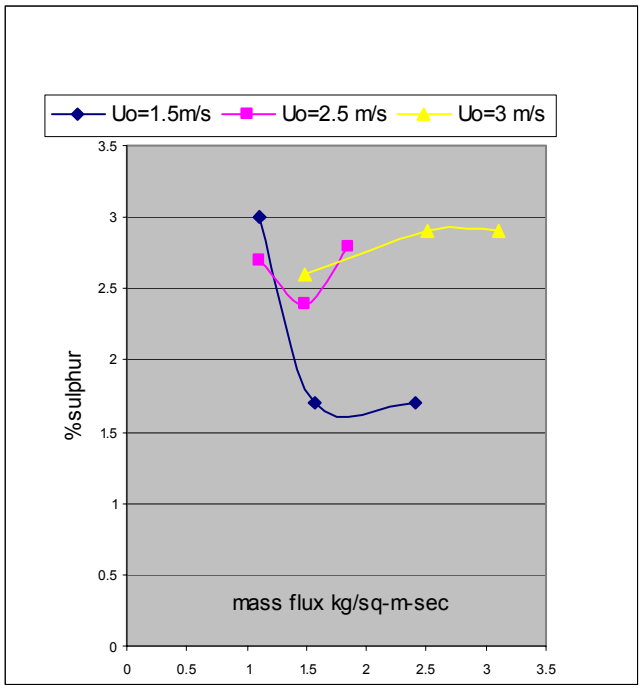

Figure 5.3.a. Percentage sulphur content in the filter for coal test. Percentage sulphur content in the initial sample is shown in Table 5.1.

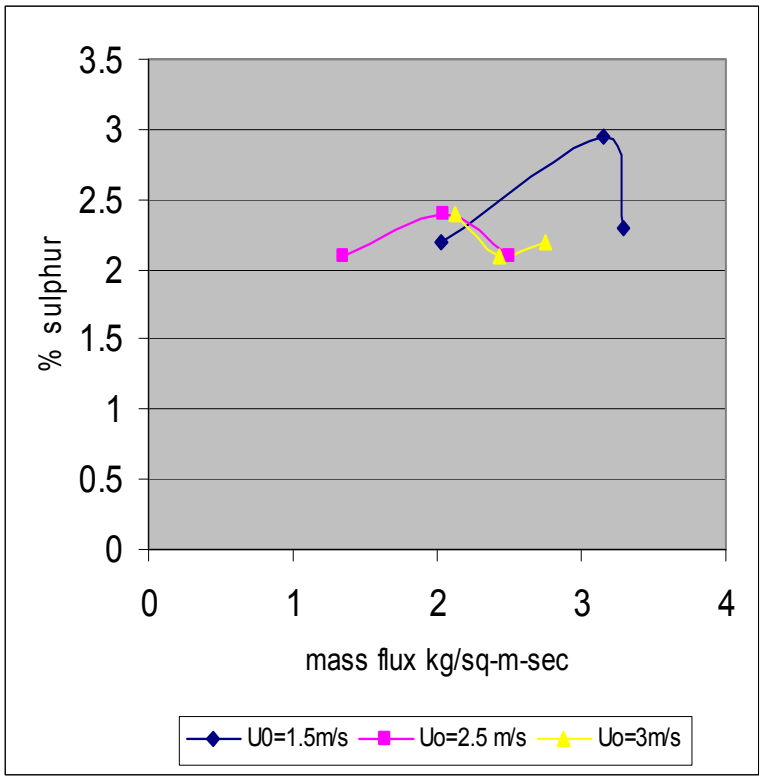

Figure 5.3.b.Percentage Sulphur content in the filter from coal/iron test. Percentage sulphur content in the initial sample is shown in Table 5.2.

The mass fraction of the clean coal was defined as follows.

$$\text{Mass fraction of clean coal } \emptyset = \frac{\text{Mass of coal in the filter}}{\text{(Total mass of coal introduced in the system)}} * 100$$

Figure 5.3.c and 5.3.d show the mass fraction of clean coal for different test conditions.

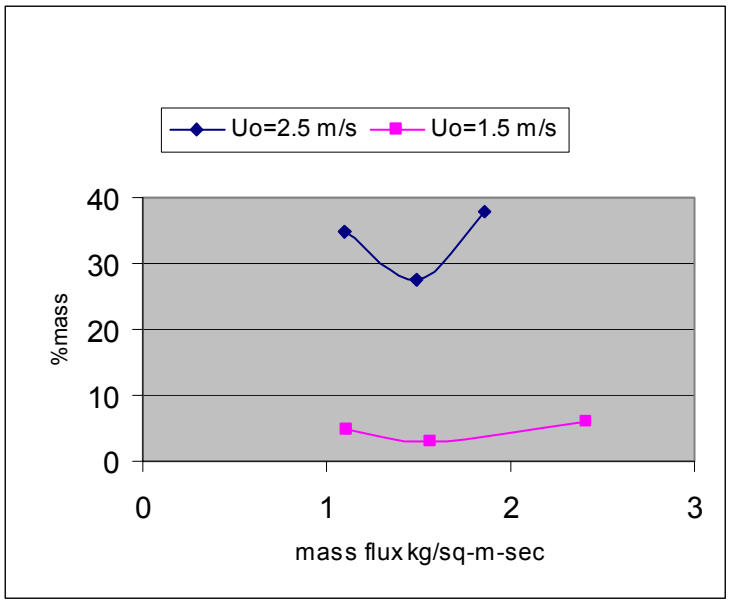

Figure 5.3.c. Mass fraction of clean coal for coal tests

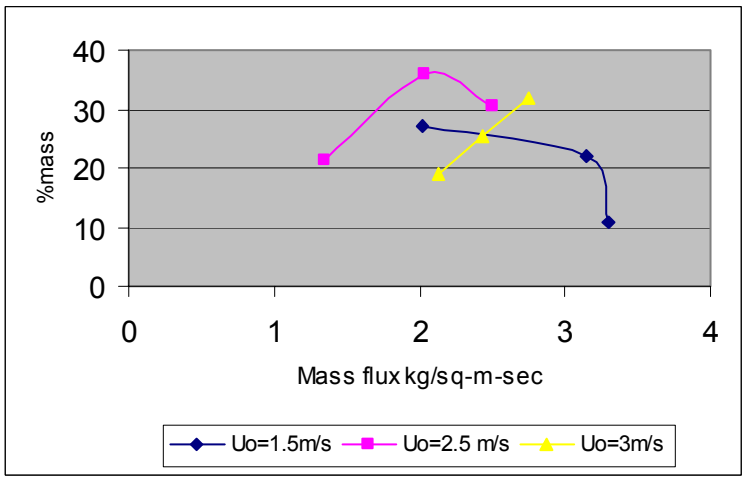

Figure 5.3.d Mass fraction of clean coal for coal/iron tests.

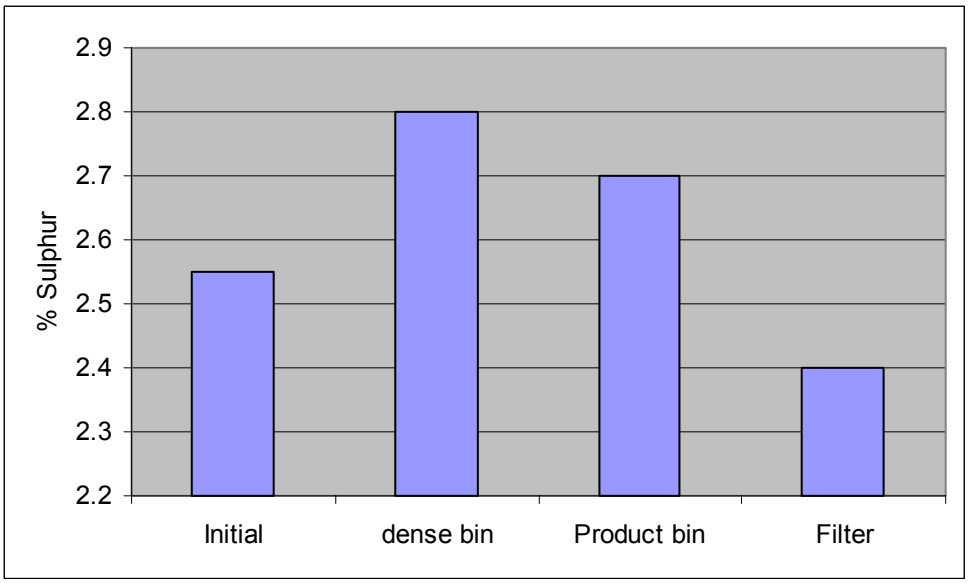

Figure 5.3.e. Percentage Sulphur in each bin for test 4 (G=1.4858 kg/m2-s, Uo=2.5m/s)

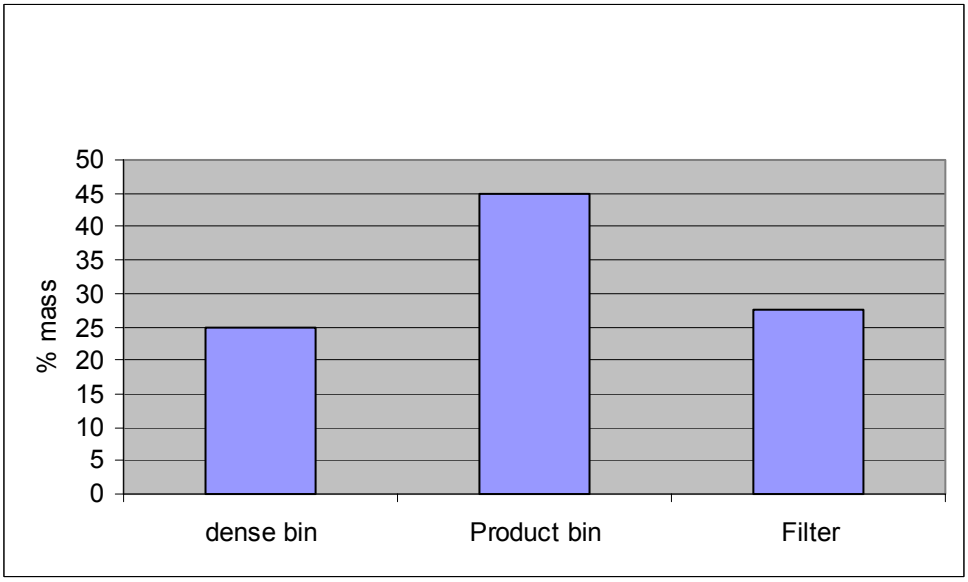

Figure 5.3.f. Percentage Mass in each bin for test 4 (G=1.4858 kg/m2-s, Uo=2.5m/s)

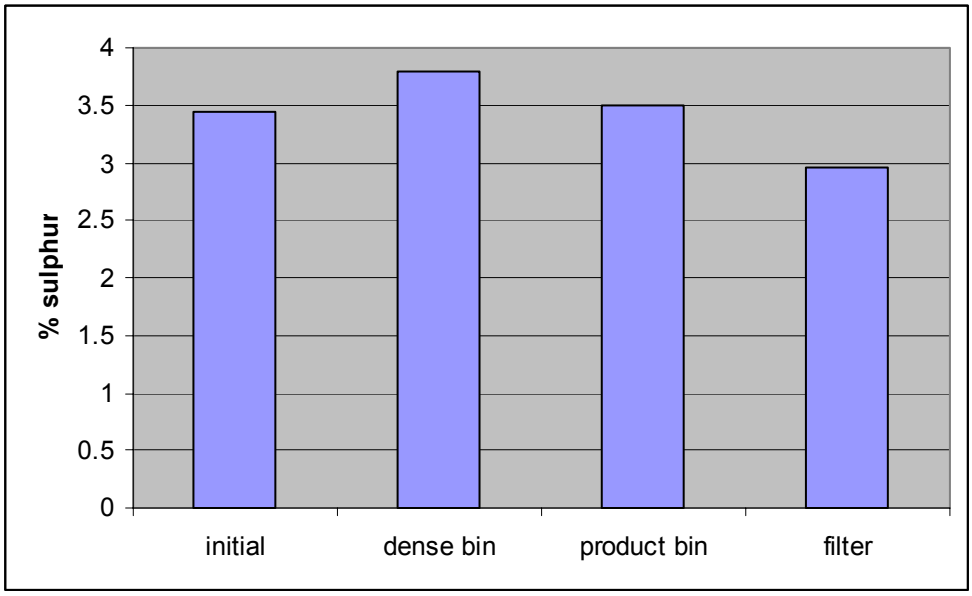

Figure 5.3.g. Percentage sulphur in each bin for test 16 (G=3.1502 kg/m2-s, Uo=1.5m/s)

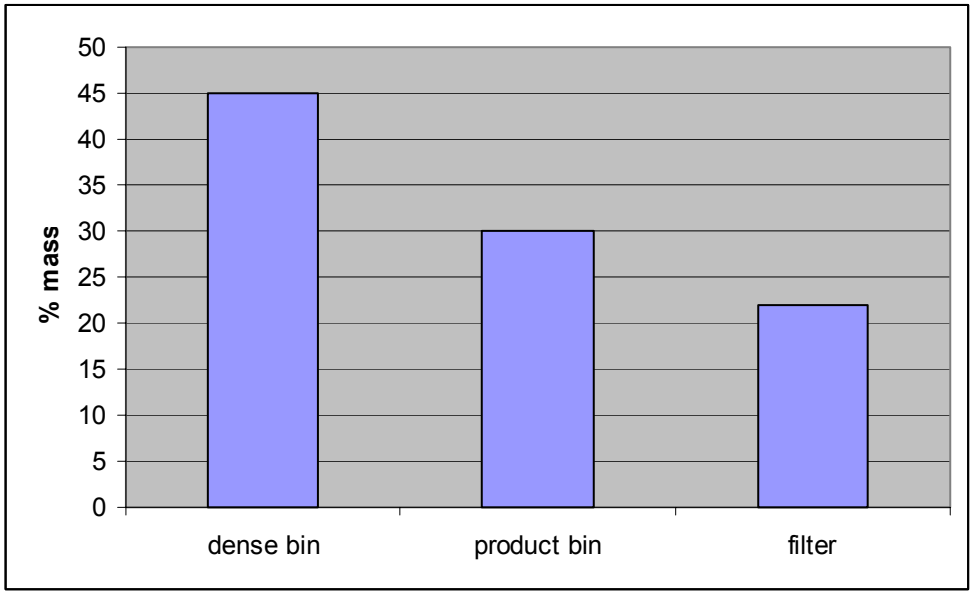

Figure 5.3.h. Percentage mass in each bin for test 16 (G=3.1502 kg/m2-s, Uo=1.5m/s)

5.4 Electronic Scanning Microscope Image

Microscopic images of the coal particles in the filter were taken. One of the images is shown in Figure 5.4. These pictures also gave an indication of the size distribution range of solids collected in the filter. In test 5 run at a superficial velocity of 2.5 m/s and mass flux of 1.0982 kg/m^2-s, the majority of the particles were in the size range of 5-25 micrometers. However, there were some particles with a size of 200 micrometers as well. Most of the solid particles collected in the filter were larger than the cut off size of the cyclones. Figure 4.2.a. shows that for this test, the cyclone efficiency was 52%.

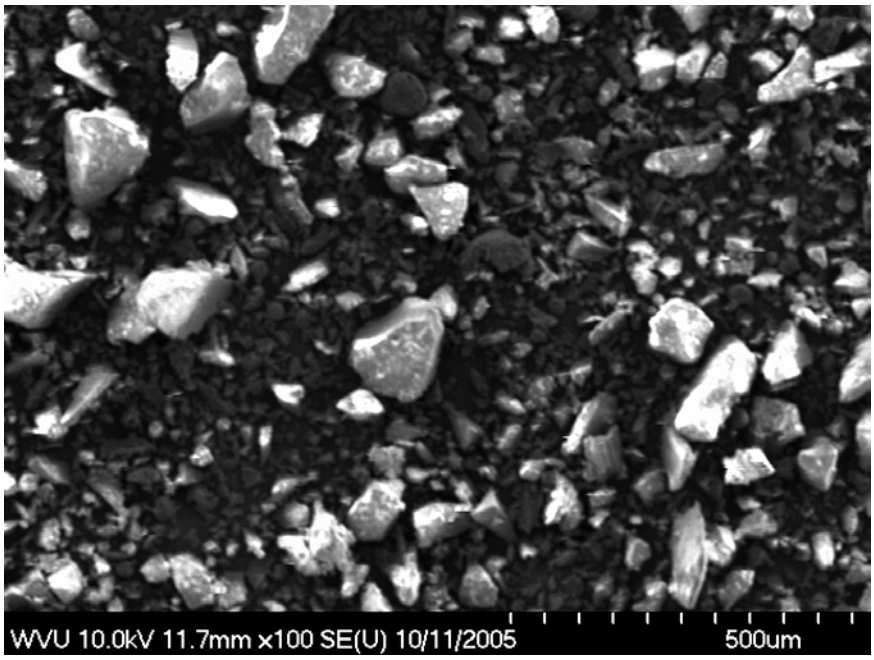

Figure 5.4 Electron Microscopic Image of solids in Filter

CHAPTER 6

CONCLUSIONS AND RECOMMENDATIONS

6.1 Conclusions

The goal of this study was to design and investigate a dry separation system with the capability of fluidizing particles in the 0-150 micrometer range i.e. A and C class particles. This system was to remove pyritic sulphur from coal fines. In this study, different pneumatic injection schemes for transport of solids from the feed hopper to the riser were studied.

From the data gathered during testing, it was concluded that feed configuration A resulted in a steady state flow of solids from the feed hopper to the riser. In feed configuration C, solids were settling in the horizontal pipe and clogging it resulting in no flow of solids to the riser. In feed configuration B, recirculating the air from the primary cyclone back to the feed hopper resulted in reduction of the flow stoppage of the solids to the riser but steady state was not achieved.

This series of testing was conducted at superficial velocities higher than the terminal velocity of coal and pyrite in the 0-150 micrometer size range. Testing at lower superficial velocities could not be conducted because the solid particles started to clog the horizontal section of the three feeder configurations for low air flow rates supplied to them.

Sulphur content was insignificantly lowered in the coal collected in the filter for superficial velocities of 1.5 m/s and 2.5 m/s for the pure coal tests. The mass collected in the filter bin was in the range of 3% to 38% of the initial mass in the system. For test 14 run at a superficial velocity of 1.5 m/s and a mass flux of 1.56 kg/m^2-s, sulphur content in the coal collected in the filter was only 1.7% by mass as compared to 3.05 % sulphur by mass in the initial coal sample but only 3% of the initial mass ended up in the filter.

Adding iron to the coal particles resulted in insignificant separation of pyrite from coal at all superficial velocities. In these tests, increasing the superficial velocity from 1.5 m/s to 2.5 m/s resulted in an increase in the mass fraction of coal particles collected in the filter bin as shown in Figure 5.3.d.

No practical observation of the force of adhesion between iron and pyrite was found in this study.

This system has shown that removing pyrite from fine coal using a dry separation method may be possible but further testing at lower superficial velocities closer to the terminal velocity of fine coal particles will be required to decrease the percentage mass content of sulphur in coal and to increase the mass fraction of the clean coal.

6.2 Recommendations

The system produced insignificant separation of coal from pyrite. There was room for more improvements that could be made in the future.

Tests at lower air flow rate and lower superficial velocities should be conducted so that the superficial velocity is lower than the terminal velocity of coal particles. Since pyrite is denser than coal, lighter coal particles would be carried out of the riser by the air while denser pyrite particles could be collected in the dense bin. A mechanism had to be devised so that the solid particles did not clog the pneumatic injection system for low air flow rates. Multiple air injections in the horizontal portion of the feeder configuration could help with the steady flow of the solids to the riser. Better filter bags were needed that do not rupture easily.

The location of the test stand itself should be changed and be brought in front of the larger fluidized riser system in the High Bay area of NRCCE. This would help in better visual inspection of the solids in the riser.

REFERENCES

Banhart,J. and Knuwer,M.(1998), " Powder Injection and Formation of Porosity in Spray Forming", PM World Congress.

Baeyens, J. and Geldart, D.(1978), " Particle Mixing in Gas-Fluidized Bed", La Fluidization et sas Applications.

Buisman, Rein (2000), "Fine Coal Screening using Pensep Screen", Coal Prep Show.

Desautels, R.L. (2005), "Theory of van der Waals Forces as Applied to Particulate Materials", Educational resources for Particle Technology.

Ergun,S.(1952), "Fluid Flow through Packed Columns", Chem.Eng.Prog.48:89-94.

Fan, L.S. and Zhu, C. (1998), "Principles of Gas-Solid Flow", Cambridge University Press.

Hamaker, H. C. (1937), "The London-van der Waals Attraction between Spherical Particles," Physica IV, No. 10.

Hetsroni, G. (1982), "Handbook of Multiphase Systems", Hemisphere Publishing Corporation.

Hunter, R.J. (2001), "Foundations of Colloid Science", Oxford University Press.

Kunii, D. and Levenspiel, O. (1991), "Fluidization Engineering", Butterworth-Heinemann.

Li, H. and Lu,X. (2003), " Hydrodynamic Modeling of the L-Valve", Powder Technology, 129: 8-14.

Lim,K.S, Zhu,J.X. and Grace, J.R.(1995), " Hydrodynamics of Gas-Solid Fluidization", Int.J.Multiphase Flow, 21:141-193.

Regester, J.L (2004), "Separation of Small Particles due to Density Differences in a CFB Riser System". Thesis, West Virginia University.

Rhodes,M. (2001), " Fluidization of Particles by Fluids", Educational resources for Particle Technology.

Trivedi,A and Sud,V.K. (2002), "Grain Characteristics and Engineering Properties of Coal Ash" , Granular Matter 4:93-101.

Wen,C.Y. and Yu,Y.H.(1966), " Generalized Method of Predicting Minimum Fluidization Velocity", AIChE J. 12:610-612.

Yang, H. (1995), "Experimental Study on the Hydrodynamics in the Riser of a Circulating Fluidized Bed", Dissertation, West Virginia University.

Yerushalami, J. and Turner, D.H. (1976), " The Fast Fluidized Bed", Ind. Eng. Chem. Process Des. Dev. 15:47-53.

APPENDIX

A1: Elemental Analysis

Summarize Results

Date :	9/28/05	09:51:14
Method Name :	NCHS	
Method Filename :	092705.mth	

Group No : 1	Element %			
Sample Name	Nitrogen%	Carbon%	Hydrogen%	Sulphur%
Test 4 Dense Bin	1.383410692	71.92733765	5.236793041	2.810038328
Test 4 Dense Bin	1.342687249	71.67329407	5.256966114	2.840862989
Test 4 Dense Bin	1.360520959	71.55602264	5.23795557	2.920008659

3 Sample(s) in Group No : 1

Component Name	Average	Std. Dev.	% Rel. S. D.	Variance
Nitrogen%	1.3622063	0.02041396	1.4986	0.0004
Carbon%	71.71888479	0.1898094	0.2647	0.036
Hydrogen%	5.243904908	0.01132626	0.216	0.0001
Sulphur%	2.856969992	0.05672694	1.9856	0.0032

Group No : 2	Element %			
Sample Name	Nitrogen%	Carbon%	Hydrogen%	Sulphur%
Test 4 Product Bin	1.353066921	71.7435379	5.180651665	2.684589148
Test 4 Product Bin	1.34987843	71.65248871	5.192575455	2.71036768
Test 4 Product Bin	1.301071525	72.02198792	5.184790611	2.646798372

3 Sample(s) in Group No : 2

Component Name	Average	Std. Dev.	% Rel. S. D.	Variance
Nitrogen%	1.334672292	0.02914276	2.1835	0.0008
Carbon%	71.80600484	0.1925072	0.2681	0.0371
Hydrogen%	5.18600591	0.006054081	0.1167	0
Sulphur%	2.680585066	0.03197325	1.1928	0.001

Group No : 3	Element %			
Sample Name	Nitrogen%	Carbon%	Hydrogen%	Sulphur%
Test 4 Filter	1.383721471	72.59542084	5.230240822	2.410982609
Test 4 Filter	1.309272766	72.47797394	5.199998379	2.409651995
Test 4 Filter	1.348000884	72.56790161	5.230540276	2.523099422

3 Sample(s) in Group No : 3

Component Name	Average	Std. Dev.	% Rel. S. D.	Variance
Nitrogen%	1.346998374	0.03723447	2.7643	0.0014
Carbon%	72.5470988	0.06142484	0.0847	0.0038
Hydrogen%	5.220259825	0.01754757	0.3361	0.0003
Sulphur%	2.447911342	0.06511819	2.6602	0.0042

Group No : 4	Element %			
Sample Name	Nitrogen%	Carbon%	Hydrogen%	Sulphur%
Test 5 Dense bin	1.461956739	73.41378784	5.339493752	2.89056015
Test 5 Dense bin	1.476360798	73.03756714	5.353217125	2.457556248
Test 5 Dense bin	1.476942301	73.3274765	5.416394234	3.052058935

3 Sample(s) in Group No : 4

Component Name	Average	Std. Dev.	% Rel. S. D.	Variance
Nitrogen%	1.471753279	0.008489033	0.5768	0.0001
Carbon%	73.25961049	0.1970783	0.269	0.0388
Hydrogen%	5.369701703	0.04101496	0.7638	0.0017
Sulphur%	2.800058444	0.3074106	10.9787	0.0945

Group No : 5	Element %			
Sample Name	Nitrogen%	Carbon%	Hydrogen%	Sulphur%
Test 5 Product bin	1.520661235	72.22888947	5.25547123	3.14107132
Test 5 Product bin	1.463148236	71.87010193	5.198663712	3.006993294
Test 5 Product bin	1.462616324	71.570755	5.191411972	3.170191288

3 Sample(s) in Group No : 5

Component Name	Average	Std. Dev.	% Rel. S. D.	Variance
Nitrogen%	1.482141932	0.03335975	2.2508	0.0011
Carbon%	71.88991547	0.3295143	0.4584	0.1086
Hydrogen%	5.215182304	0.03507913	0.6726	0.0012
Sulphur%	3.1060853	0.08704259	2.8023	0.0076

Group No : 6	Element %			
Sample Name	Nitrogen%	Carbon%	Hydrogen%	Sulphur%
Test 5 Filter	1.441868305	72.68723297	5.219290257	2.60001421
Test 5 Filter	1.433173537	72.23778534	5.193168163	2.791906834
Test 5 Filter	1.456254363	71.97612762	5.129765511	2.59480691

3 Sample(s) in Group No : 6

Component Name	Average	Std. Dev.	% Rel. S. D.	Variance
Nitrogen%	1.443765402	0.01165677	0.8074	0.0001
Carbon%	72.30038198	0.3596616	0.4975	0.1294
Hydrogen%	5.18074131	0.04603792	0.8886	0.0021
Sulphur%	2.662242651	0.1123227	4.2191	0.0126

Group No : 7	Element %			
Sample Name	Nitrogen%	Carbon%	Hydrogen%	Sulphur%
Test 6 Dense bin	1.48559761	73.00745392	5.344347477	2.837650061
Test 6 Dense bin	1.540419936	72.71612549	5.347622871	2.919233084
Test 6 Dense bin	1.448377252	73.0320816	5.324394226	2.900500059

3 Sample(s) in Group No : 7

Component Name	Average	Std. Dev.	% Rel. S. D.	Variance
Nitrogen%	1.491464933	0.046301	3.1044	0.0021
Carbon%	72.91855367	0.1757399	0.241	0.0309
Hydrogen%	5.338788191	0.01257266	0.2355	0.0002
Sulphur%	2.885794401	0.04273336	1.4808	0.0018

Group No : 8	Element %			
Sample Name	Nitrogen%	Carbon%	Hydrogen%	Sulphur%
Test 6 Product bin	1.636533737	72.58009338	5.239276886	2.637305975
Test 6 Product bin	1.521860361	72.81749725	5.235352993	2.62666297
Test 6 Product bin	1.654873729	72.7134552	5.211714745	2.673918486

3 Sample(s) in Group No : 8

Component Name	Average	Std. Dev.	% Rel. S. D.	Variance
Nitrogen%	1.604422609	0.07208663	4.493	0.0052
Carbon%	72.70368195	0.1190033	0.1637	0.0142
Hydrogen%	5.228781541	0.01490993	0.2852	0.0002
Sulphur%	2.645962477	0.02478855	0.9368	0.0006

Group No : 9	Element %			
Sample Name	Nitrogen%	Carbon%	Hydrogen%	Sulphur%
Test 6 Filter	1.93785131	72.42539978	5.208659649	2.712680101
Test 6 Filter	1.743192673	72.09745789	5.176829815	2.843706608
Test 6 Filter	1.690754652	72.65479279	5.159376144	2.68369627

3 Sample(s) in Group No : 9

Component Name	Average	Std. Dev.	% Rel. S. D.	Variance
Nitrogen%	1.790599545	0.1301912	7.2708	0.0169
Carbon%	72.39255015	0.2801158	0.3869	0.0785
Hydrogen%	5.181621869	0.02498877	0.4823	0.0006
Sulphur%	2.746694326	0.08525581	3.1039	0.0073

Summarize
Results

Date :	10/3/05	09:33:23
Method Name :	NCHS	
Method Filename :	092805.mth	

Group No : 1	Element %			
Sample Name	Nitrogen%	Carbon%	Hydrogen%	Sulphur%
Test 7 Dense Bin	1.509539127	73.36758423	5.37282753	2.325864792
Test 7 Dense Bin	1.471816421	73.10328674	5.387971878	2.711689711
Test 7 Dense Bin	1.439796805	72.81041718	5.392238617	2.731925488

3 Sample(s) in Group No : 1

Component Name	Average	Std. Dev.	% Rel. S. D.	Variance
Nitrogen%	1.473717451	0.03491	2.3688	0.0012
Carbon%	73.09376272	0.2787056	0.3813	0.0777
Hydrogen%	5.384346008	0.01020087	0.1895	0.0001
Sulphur%	2.589826663	0.2288215	8.8354	0.0524

Group No : 2	Element %			
Sample Name	Nitrogen%	Carbon%	Hydrogen%	Sulphur%
Test 7 Product Bin	1.488156796	72.14868164	5.292497158	2.39628458
Test 7 Product Bin	1.407588005	71.76917267	5.262084007	2.904059887
Test 7 Product Bin	1.462094903	72.6689682	5.317890644	2.977674246

3 Sample(s) in Group No : 2

Component Name	Average	Std. Dev.	% Rel. S. D.	Variance
Nitrogen%	1.452613235	0.04111276	2.8303	0.0017
Carbon%	72.1956075	0.4517295	0.6257	0.2041
Hydrogen%	5.290823936	0.02794092	0.5281	0.0008
Sulphur%	2.759339571	0.3165619	11.4724	0.1002

Group No : 3	Element %			
Sample Name	Nitrogen%	Carbon%	Hydrogen%	Sulphur%
Test 7 Filter	1.503171086	73.59738922	5.376185417	2.674110889
Test 7 Filter	1.510680199	73.43178558	5.362260342	2.1673491
Test 7 Filter	1.478830934	74.0655899	5.45908308	2.463834763

3 Sample(s) in Group No : 3

Component Name	Average	Std. Dev.	% Rel. S. D.	Variance
Nitrogen%	1.49756074	0.01664935	1.1118	0.0003
Carbon%	73.6982549	0.3287208	0.446	0.1081
Hydrogen%	5.39917628	0.05234592	0.9695	0.0027
Sulphur%	2.435098251	0.2546001	10.4554	0.0648

Group No : 4	Element %			
Sample Name	Nitrogen%	Carbon%	Hydrogen%	Sulphur%
Test 8 Dense Bin	1.372876287	62.40401077	4.625261307	2.00190258
Test 8 Dense Bin	1.284443855	59.73305893	4.485188961	1.824262738
Test 8 Dense Bin	1.368732452	60.62131119	4.501391888	2.20486927

3 Sample(s) in Group No : 4

Component Name	Average	Std. Dev.	% Rel. S. D.	Variance
Nitrogen%	1.342017531	0.0499033	3.7185	0.0025
Carbon%	60.9194603	1.360208	2.2328	1.8502
Hydrogen%	4.537280718	0.07662292	1.6887	0.0059
Sulphur%	2.010344863	0.1904436	9.4732	0.0363

Group No : 5	Element %			
Sample Name	Nitrogen%	Carbon%	Hydrogen%	Sulphur%
Test 8 Product Bin	1.392293215	65.06745148	4.762853622	1.792905569
Test 8 Product Bin	1.330281377	62.26226425	4.570716858	1.918668747
Test 8 Product Bin	1.292465448	62.96015549	4.613641262	2.119090557

3 Sample(s) in Group No : 5

Component Name	Average	Std. Dev.	% Rel. S. D.	Variance
Nitrogen%	1.33834668	0.05040022	3.7659	0.0025
Carbon%	63.42995707	1.460412	2.3024	2.1328
Hydrogen%	4.649070581	0.1008492	2.1692	0.0102
Sulphur%	1.943554958	0.1645104	8.4644	0.0271

Group No : 6	Element %			
Sample Name	Nitrogen%	Carbon%	Hydrogen%	Sulphur%
Test 8 Filter	1.453237057	68.74633026	4.985345364	2.104366302
Test 8 Filter	1.315839648	67.83540344	4.936355114	2.276741743
Test 8 Filter	1.280738711	67.03165436	4.901865482	2.268339634

3 Sample(s) in Group No : 6

Component Name	Average	Std. Dev.	% Rel. S. D.	Variance
Nitrogen%	1.349938472	0.09116451	6.7532	0.0083
Carbon%	67.87112935	0.857896	1.264	0.736
Hydrogen%	4.941188653	0.04194931	0.849	0.0018
Sulphur%	2.21648256	0.09718637	4.3847	0.0094

Group No : 7	Element %			
Sample Name	Nitrogen%	Carbon%	Hydrogen%	Sulphur%
Test 9 Dense Bin	1.45314908	72.44656372	5.339794159	2.583412409
Test 9 Dense Bin	1.447977304	71.76182556	5.343635082	2.749439001
Test 9 Dense Bin	1.250611544	71.16369629	5.290385246	2.518536806

3 Sample(s) in Group No : 7

Component Name	Average	Std. Dev.	% Rel. S. D.	Variance
Nitrogen%	1.383912643	0.1154711	8.3438	0.0133
Carbon%	71.79069519	0.6419208	0.8942	0.4121
Hydrogen%	5.324604829	0.02969719	0.5577	0.0009
Sulphur%	2.617129405	0.1190865	4.5503	0.0142

Group No : 8	Element %			
Sample Name	Nitrogen%	Carbon%	Hydrogen%	Sulphur%
Test 9 Product Bin	1.362012982	72.28160858	5.329547882	1.893508792

Test 9 Product Bin	1.436575294	72.90631866	5.287792683	2.480980158
Test 9 Product Bin	1.394633174	72.46965027	5.272368908	2.390084743

3 Sample(s) in Group No : 8

Component Name	Average	Std. Dev.	% Rel. S. D.	Variance
Nitrogen%	1.397740483	0.03737815	2.6742	0.0014
Carbon%	72.55252584	0.3204948	0.4417	0.1027
Hydrogen%	5.296569824	0.02958272	0.5585	0.0009
Sulphur%	2.254857898	0.3162205	14.024	0.1

Group No : 9	Element %			
Sample Name	Nitrogen%	Carbon%	Hydrogen%	Sulphur%
Test 9 Filter	1.469017982	72.81808472	5.301596165	2.029809475
Test 9 Filter	1.413799763	72.4355545	5.256879807	2.278017282
Test 9 Filter	1.370548487	72.78137207	5.301329136	1.856143236

3 Sample(s) in Group No : 9

Component Name	Average	Std. Dev.	% Rel. S. D.	Variance
Nitrogen%	1.417788744	0.04935579	3.4812	0.0024
Carbon%	72.6783371	0.2110557	0.2904	0.0445
Hydrogen%	5.286601702	0.02574026	0.4869	0.0007
Sulphur%	2.054656665	0.2120318	10.3196	0.045

Summarize Results

Date :	10/5/05	09:57:16
Method Name :	NCHS	
Method Filename :	100405.mth	

Group No : 1	Element %			
Sample Name	Nitrogen%	Carbon%	Hydrogen%	Sulphur%
Test 12 Filter	1.268012881	70.36379242	4.834600925	2.690269232
Test 12 Filter	1.213950276	70.38541412	4.882401466	3.033809423
Test 12 Filter	1.29325974	70.50772095	4.882510185	2.761839151

3 Sample(s) in Group No : 1

Component Name	Average	Std. Dev.	% Rel. S. D.	Variance
Nitrogen%	1.258407633	0.04051781	3.2198	0.0016
Carbon%	70.41897583	0.07761215	0.1102	0.006
Hydrogen%	4.866504192	0.02762909	0.5677	0.0008
Sulphur%	2.828639269	0.1812503	6.4077	0.0329

Group No : 2	Element %			
Sample Name	Nitrogen%	Carbon%	Hydrogen%	Sulphur%
Test 13 Dense Bin	1.233153343	69.25615692	4.760125637	2.823290348
Test 13 Dense Bin	1.32550931	67.70528412	4.693337917	2.95236516

Test 13 Dense Bin	1.20255506	67.50095367	4.755730152	3.500855446

3 Sample(s) in Group No : 2

Component Name	Average	Std. Dev.	% Rel. S. D.	Variance
Nitrogen%	1.253739238	0.06400993	5.1055	0.0041
Carbon%	68.15413157	0.9598347	1.4083	0.9213
Hydrogen%	4.736397902	0.03735575	0.7887	0.0014
Sulphur%	3.092170318	0.3597676	11.6348	0.1294

Group No : 3	Element %			
Sample Name	Nitrogen%	Carbon%	Hydrogen%	Sulphur%
Test 13 Product Bin	1.264253855	69.66906738	4.844721794	3.494969368
Test 13 Product Bin	1.316447377	69.09359741	4.806184769	3.657897711
Test 13 Product Bin	1.252461791	69.55474091	4.84963274	3.347599268

3 Sample(s) in Group No : 3

Component Name	Average	Std. Dev.	% Rel. S. D.	Variance
Nitrogen%	1.277721008	0.03405234	2.6651	0.0012
Carbon%	69.43913523	0.3046554	0.4387	0.0928
Hydrogen%	4.833513101	0.02379407	0.4923	0.0006
Sulphur%	3.500155449	0.1552142	4.4345	0.0241

Group No : 4	Element %			
Sample Name	Nitrogen%	Carbon%	Hydrogen%	Sulphur%
Test 13 Filter	1.309181094	70.71411896	4.891971588	2.769627571
Test 13 Filter	1.229451299	70.62364197	4.846307755	2.725801945
Test 13 Filter	1.334105849	70.98927307	4.928555012	2.6963346

3 Sample(s) in Group No : 4

Component Name	Average	Std. Dev.	% Rel. S. D.	Variance
Nitrogen%	1.290912747	0.05466665	4.2347	0.003
Carbon%	70.775678	0.1904302	0.2691	0.0363
Hydrogen%	4.888944785	0.04120709	0.8429	0.0017
Sulphur%	2.730588039	0.03688014	1.3506	0.0014

Group No : 5	Element %			
Sample Name	Nitrogen%	Carbon%	Hydrogen%	Sulphur%
Test 14 Dense Bin	1.413191438	70.67321777	5.007552147	3.243761301
Test 14 Dense Bin	1.458823323	70.67993927	4.967416286	3.473249197
Test 14 Dense Bin	1.403738737	70.70864105	5.003481865	3.379703045

3 Sample(s) in Group No : 5

Component Name	Average	Std. Dev.	% Rel. S. D.	Variance
Nitrogen%	1.425251166	0.029456	2.0667	0.0009
Carbon%	70.68726603	0.01881391	0.0266	0.0004
Hydrogen%	4.992816766	0.0220914	0.4425	0.0005
Sulphur%	3.365571181	0.1153948	3.4287	0.0133

Group No : 6	Element %			
Sample Name	Nitrogen%	Carbon%	Hydrogen%	Sulphur%
Test 14 Product Bin	1.406256795	71.54325104	5.052244186	3.158814907
Test 14 Product Bin	1.450043917	71.27407074	5.063240528	3.174591541
Test 14 Product Bin	1.406843901	71.47325134	4.994798183	2.80600667

3 Sample(s) in Group No : 6

Component Name	Average	Std. Dev.	% Rel. S. D.	Variance
Nitrogen%	1.421048204	0.02511274	1.7672	0.0006
Carbon%	71.43019104	0.1396608	0.1955	0.0195
Hydrogen%	5.036760966	0.0367544	0.7297	0.0014
Sulphur%	3.046471039	0.2083976	6.8406	0.0434

Group No : 7	Element %			
Sample Name	Nitrogen%	Carbon%	Hydrogen%	Sulphur%
Test 14 Filter	1.400832891	70.68874359	4.889823914	2.428311348
Test 14 Filter	1.347060919	70.38718414	4.8586092	2.001527071
Test 14 Filter	1.384444237	70.81596375	4.887052536	2.36724925

3 Sample(s) in Group No : 7

Component Name	Average	Std. Dev.	% Rel. S. D.	Variance
Nitrogen%	1.377446016	0.02756062	2.0008	0.0008
Carbon%	70.63063049	0.2202177	0.3118	0.0485
Hydrogen%	4.878495216	0.01727745	0.3542	0.0003
Sulphur%	2.26569589	0.2308052	10.1869	0.0533

Group No : 8	Element %			
Sample Name	Nitrogen%	Carbon%	Hydrogen%	Sulphur%
Test 15 Dense Bin	1.441047668	71.09718323	5.062261581	3.453870773
Test 15 Dense Bin	1.449050307	71.61833191	5.069014549	3.594012022
Test 15 Dense Bin	1.455947518	72.09318542	5.089220524	3.115469694

3 Sample(s) in Group No : 8

Component Name	Average	Std. Dev.	% Rel. S. D.	Variance
Nitrogen%	1.448681831	0.007456756	0.5147	0.0001
Carbon%	71.60290019	0.4981804	0.6958	0.2482

Hydrogen%	5.073498885	0.01402776	0.2765	0.0002
Sulphur%	3.387784163	0.2460209	7.262	0.0605

Group No : 9	Element %			
Sample Name	Nitrogen%	Carbon%	Hydrogen%	Sulphur%
Test 15 Product Bin	1.460393429	72.20628357	5.078221321	2.93350935
Test 15 Product Bin	1.442703605	72.41331482	5.082350254	2.787406206
Test 15 Product Bin	1.379415989	72.84089661	5.064082146	2.999495506

3 Sample(s) in Group No : 9

Component Name	Average	Std. Dev.	% Rel. S. D.	Variance
Nitrogen%	1.427504341	0.04257464	2.9825	0.0018
Carbon%	72.48683167	0.3236309	0.4465	0.1047
Hydrogen%	5.074884574	0.009580259	0.1888	0.0001
Sulphur%	2.906803687	0.1085374	3.7339	0.0118

Group No : 10	Element %			
Sample Name	Nitrogen%	Carbon%	Hydrogen%	Sulphur%
Test 15 Filter	1.293303013	68.41333771	4.681838036	2.109983206
Test 15 Filter	1.234290838	68.10063934	4.666471481	2.063625336
Test 15 Filter	1.26977098	68.16944122	4.692348957	2.0861938

3 Sample(s) in Group No : 10

Component Name	Average	Std. Dev.	% Rel. S. D.	Variance
Nitrogen%	1.265788277	0.029707	2.3469	0.0009
Carbon%	68.22780609	0.1643165	0.2408	0.027
Hydrogen%	4.680219491	0.01301444	0.2781	0.0002
Sulphur%	2.08660078	0.02318162	1.111	0.0005

Summarize Results

Date :	10/7/05	15:33:51
Method Name :	NCHS	
Method Filename :	100705.mth	

Group No : 1	Element %			
Sample Name	Nitrogen%	Carbon%	Hydrogen%	Sulphur%
Test 19 Dense Bin	1.721116662	72.14743042	5.076706409	2.917324305
Test 19 Dense Bin	1.784106612	72.85870361	5.171872616	2.935624361
Test 19 Dense Bin	1.729912281	73.31252289	5.182426929	2.880396605

3 Sample(s) in Group No : 1

Component Name	Average	Std. Dev.	% Rel. S. D.	Variance
Nitrogen%	1.745045185	0.03411286	1.9548	0.0012
Carbon%	72.77288564	0.5872679	0.807	0.3449

Hydrogen%	5.143668652	0.05823062	1.1321	0.0034
Sulphur%	2.91111509	0.02813258	0.9664	0.0008

Group No : 2	Element %			
Sample Name	Nitrogen%	Carbon%	Hydrogen%	Sulphur%
Test 19 Product Bin	1.773334265	73.6674881	5.129414558	2.631607533
Test 19 Product Bin	1.778420925	74.61585236	5.197183609	2.517170191
Test 19 Product Bin	1.615058303	73.06075287	5.069981575	2.638380289

3 Sample(s) in Group No : 2

Component Name	Average	Std. Dev.	% Rel. S. D.	Variance
Nitrogen%	1.722271164	0.09288388	5.3931	0.0086
Carbon%	73.78136444	0.783779	1.0623	0.6143
Hydrogen%	5.132193247	0.06364653	1.2401	0.0041
Sulphur%	2.595719337	0.0681098	2.6239	0.0046

Group No : 3	Element %			
Sample Name	Nitrogen%	Carbon%	Hydrogen%	Sulphur%
Test 19 Filter	1.665755391	72.66481781	4.934632301	2.30689764
Test 19 Filter	1.706292033	72.35983276	4.978608608	2.461787701
Test 19 Filter	1.705620408	72.44789124	4.993014812	2.498811722

3 Sample(s) in Group No : 3

Component Name	Average	Std. Dev.	% Rel. S. D.	Variance
Nitrogen%	1.692555944	0.02321239	1.3714	0.0005
Carbon%	72.49084727	0.1569646	0.2165	0.0246
Hydrogen%	4.968751907	0.03041374	0.6121	0.0009
Sulphur%	2.422499021	0.1018109	4.2027	0.0104

Group No : 4	Element %			
Sample Name	Nitrogen%	Carbon%	Hydrogen%	Sulphur%
Test 20 Dense Bin	1.827266574	73.74200439	5.156167507	2.553376436
Test 20 Dense Bin	1.729706764	73.84792328	5.165931225	2.542384624
Test 20 Dense Bin	1.734346509	73.51574707	5.091386795	2.316596031

3 Sample(s) in Group No : 4

Component Name	Average	Std. Dev.	% Rel. S. D.	Variance
Nitrogen%	1.763773282	0.05503572	3.1203	0.003
Carbon%	73.70189158	0.1696822	0.2302	0.0288
Hydrogen%	5.137828509	0.0405149	0.7886	0.0016
Sulphur%	2.470785697	0.1336452	5.409	0.0179

Summarize
Results

Date :	10/11/05	09:47:52
Method Name :	NCHS	
Method Filename :	100905.mth	

Group No : 1	Element %			
Sample Name	Nitrogen%	Carbon%	Hydrogen%	Sulphur%
Test 20 Product Bin	1.397323132	72.67690277	4.978422165	2.618671656
Test 20 Product Bin	1.427046657	73.19421387	5.051533222	2.50910449
Test 20 Product Bin	1.45800364	73.17240906	5.046986103	2.484194756

3 Sample(s) in Group No : 1

Component Name	Average	Std. Dev.	% Rel. S. D.	Variance
Nitrogen%	1.427457809	0.03034234	2.1256	0.0009
Carbon%	73.01450857	0.2925784	0.4007	0.0856
Hydrogen%	5.025647163	0.04096119	0.815	0.0017
Sulphur%	2.537323634	0.07154194	2.8196	0.0051

Group No : 2	Element %			
Sample Name	Nitrogen%	Carbon%	Hydrogen%	Sulphur%
Test 20 Filter	1.418485999	71.79325104	4.939137459	2.192841768
Test 20 Filter	1.333402395	72.27298737	4.968900204	2.165972948
Test 20 Filter	1.386303186	72.18543243	4.918292522	2.177430153

3 Sample(s) in Group No : 2

Component Name	Average	Std. Dev.	% Rel. S. D.	Variance
Nitrogen%	1.379397194	0.04296015	3.1144	0.0018
Carbon%	72.08389028	0.2554796	0.3544	0.0653
Hydrogen%	4.942110062	0.02543446	0.5146	0.0006
Sulphur%	2.17874829	0.01348282	0.6188	0.0002

Group No : 3	Element %			
Sample Name	Nitrogen%	Carbon%	Hydrogen%	Sulphur%
Test 21 Dense Bin	1.447735548	72.41567993	5.088441849	3.021961451
Test 21 Dense Bin	1.416027427	72.32047272	5.098917007	3.067577362
Test 21 Dense Bin	1.34030652	72.67719269	5.061995983	3.286672354

3 Sample(s) in Group No : 3

Component Name	Average	Std. Dev.	% Rel. S. D.	Variance
Nitrogen%	1.401356498	0.0551967	3.9388	0.003
Carbon%	72.47111511	0.1847081	0.2549	0.0341
Hydrogen%	5.08311828	0.0190275	0.3743	0.0004
Sulphur%	3.125403722	0.1415128	4.5278	0.02

Group No : 4	Element %			
Sample Name	Nitrogen%	Carbon%	Hydrogen%	Sulphur%
Test 21 Product Bin	1.41855669	72.55167389	4.944194317	2.596086025
Test 21 Product Bin	1.379321456	72.27546692	4.965209007	2.420157433
Test 21 Product Bin	1.403231025	72.38674164	4.930284023	2.494607925

3 Sample(s) in Group No : 4

Component Name	Average	Std. Dev.	% Rel. S. D.	Variance
Nitrogen%	1.400369724	0.0197735	1.412	0.0004
Carbon%	72.40462748	0.1389694	0.1919	0.0193
Hydrogen%	4.946562449	0.01758251	0.3554	0.0003
Sulphur%	2.503617128	0.08830964	3.5273	0.0078

Group No : 5	Element %			
Sample Name	Nitrogen%	Carbon%	Hydrogen%	Sulphur%
Test 21 Filter	1.286395907	69.70142365	4.640715599	2.170721531
Test 21 Filter	1.323503852	69.6089325	4.645022869	2.08714962
Test 21 Filter	1.278241038	70.00382996	4.652813435	2.131315947

3 Sample(s) in Group No : 5

Component Name	Average	Std. Dev.	% Rel. S. D.	Variance
Nitrogen%	1.296046933	0.02412545	1.8615	0.0006
Carbon%	69.77139537	0.2065382	0.296	0.0427
Hydrogen%	4.646183968	0.006131926	0.132	0
Sulphur%	2.129729033	0.04180855	1.9631	0.0017